AD-A047 183 UNITED TECHNOLOGIES RESEARCH CENTER EAST HARTFORD CONN F/G 20/4
A METHOD FOR COMPUTING FLOWS OVER AN OGIVAL BODY.(U)
JUL 77 P R EISEMAN, R LEVY, H MCDONALD N00019-76-C-0314
UNCLASSIFIED UTRC-R77-912536-8 NL

1 OF 1
AD
A047183

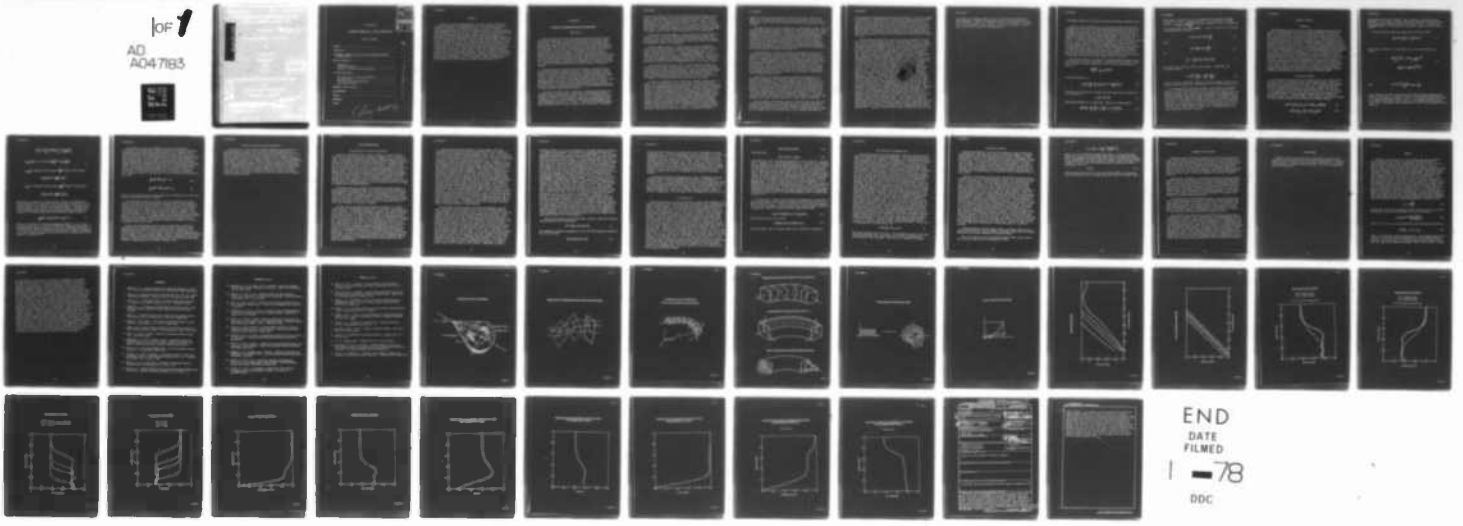

END
DATE FILMED
1-78
DDC

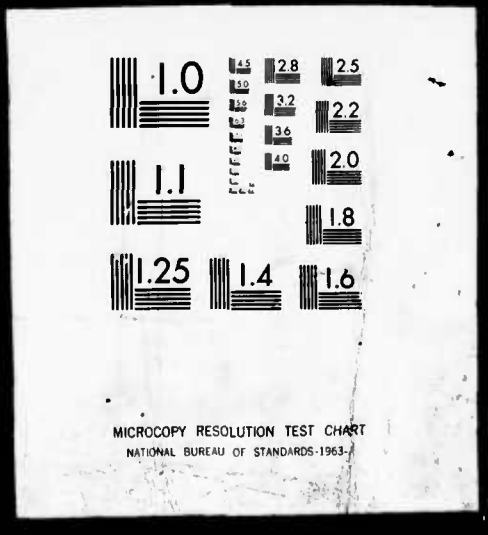

R77-912536-8

A Method for Computing Flows Over an Ogival Body

TABLE OF CONTENTS

(See 1473)

ABSTRACT

A method for computing three-dimensional flow over an ogival body at angle of attack is described. An approximate set of governing equations is given for viscous flows which have a primary flow direction. A two-level second-order accurate marching procedure is presented for general equations. With this procedure, a three-dimensional turbulent flow can be solved in any coordinate system by marching along the assumed primary flow direction. General tube-like coordinates are developed for a class of geometries applicable to flows between tubular surfaces. The coordinates are then specialized to the flow field bounded between an ogival body at angle of attack and its bow shock. Unlike the ogival body surface, the bow shock surface is not known in advance of the solution but instead must be computed as the solution develops. One marching step of the solution process is broken down into several steps. First, the bow shock surface is discretely extended by an iteration of explicit local solutions. The bow shock surface is then smoothly extended to provide a best fit to the discrete shock data. Tube-like coordinates are generated and finally the second order numerical scheme is applied to advance the fully viscous solution to the next station. In addition, some preliminary computational results were obtained. Specifically, the code was applied to subsonic boundary layers, purely supersonic flow with shocks, and mixed subsonic-supersonic flow.

A Method for Computing Flows Over an Ogival Body

INTRODUCTION

The accurate prediction of both the pressure distribution and heat transfer loads about an ogival body is an important consideration in the design of supersonic missiles. The combination of inviscid flow theory and three-dimensional boundary layer theory may be adequate to predict many flows about ogival bodies at small angles of attack; however, the separate use of these analyses are inadequate at larger angles. In such cases, a strong viscous-inviscid interaction occurs on the lee side of the body; this leads to the formation of a pair of vortices symmetric about the lee body generator. But then, under these conditions, an accurate flow field prediction requires an analysis of the mutual interaction between the viscous layer and the nominally inviscid flow. The formation of vortices will often lead to an increase in the body lift to drag ratio and in local heat transfer rate. An accurate method of predicting the interacting flow field here is necessary to insure both the effective operation and structural integrity of supersonic vehicles.

Successful predictions require an accurate flow model in which the strong viscous-inviscid coupling is modelled correctly. Boundary layer theory correctly models this coupling only when the boundary layer is closely attached to the body surface. In the case of vortex roll-up on the lee side of an ogival body at angle of attack, boundary layer theory is no longer an adequate model. Although a numerical solution to the full Navier-Stokes equations would provide a correct model, three-dimensional Navier-Stokes solutions should be used only if no suitable alternative exists. A suitable alternative should lead to accurate solutions, but should not be limited by the large running time and storage requirements associated with three-dimensional Navier-Stokes solutions.

The flow over an ogival body at incidence in a supersonic free stream can be decomposed into two distinct parts. First, there is a streamwise part which is primarily determined by inviscid mechanisms. Then there is a second part which is orthogonal to the first. This latter part accounts for the secondary flow around the body and tends to be viscous dominated. Experimental evidence supports the above decomposition (see Refs. 1, 2, 3 and 4). At zero angle of attack a symmetric flow field develops about the body, in which no cross flows exist. As the angle

of attack is increased from zero, a cross flow pattern begins to develop. As the angle is further increased, a cross flow adverse pressure gradient develops and becomes sufficiently strong to cause flow separation and then a pair of vortices symmetric about the lee symmetry plane as depicted in Fig. 1. These vortices can have imbedded shocks associated with them. The flow as depicted in Fig. 1 has been verified for both laminar and turbulent flows for speeds in the supersonic and hypersonic regimes. The available experimental data also indicates that flow separation in the axial direction usually is not associated with the vortex development.

The majority of previous attempts to predict flows of this type are numerical solutions of the inviscid flow equations, the three-dimensional boundary layer equations or both. Furthermore, the geometry was invariably restricted to conical axially symmetric bodies. Such analyses cannot predict the vortices or be applied to problems with a nontrivial body geometry.

The most common procedure is a numerical solution of the time-dependent inviscid flow equations to obtain a steady state flow field (e.g., Refs. 5 and 6). Other available inviscid techniques include the inverse method (Ref. 7) and the method of integral relations (Ref. 8). MacCormack and Warming (Ref. 9) have recently surveyed the available inviscid computational procedures. Viscous forces may in part be accounted for by making use of the inviscid pressure distribution to solve the three-dimensional boundary layer equations (see Ref. 10). The range of applicability, however, places an unacceptable restriction on the angle of attack.

At significant angles of attack, there is a need to model the complex flow field about the body with a minimal amount of effort. This effort is complicated by difficulties associated with the synthesis of inviscid flow analysis and boundary layer theory into a cohesive method of analysis. Among these difficulties are the lack of applicability of three-dimensinal boundary layer theory, a means for patching or interfacing boundary layer and rotational inviscid flow regions, and the treatment of interaction between viscous and inviscid flow regions.

In efforts to circumvent the above difficulties, Patankar & Spalding (Ref. 11), Caretto, Curr, & Spalding (Ref. 12), and Briley (Ref. 13) constructed numerical methods for solving approximate governing equations which can be viewed as a generalization of three-dimensional boundary layer theory. In these studies, solutions were computed for laminar incompressible flow in straight ducts with rectangular cross sections. The governing equations were solved by integrating in a primary flow coordinate direction while retaining viscous stresses in <u>both</u> transverse coordinate directions as opposed to only one direction for three-dimensional boundary layer theory. In addition, the pressure gradient terms were given special treatment to permit solution by forward marching integration. Subsequently, this general approach has been used to compute laminar incompressible flow in helical tubes by Patankar, Pratap & Spalding (Ref. 14). A predictor/corrector solution procedure has been developed Lin and Rubin (Refs. 15 and 16) to solve the approximate three-dimensional compressible Navier-Stokes equations. The numerical technique is

implicit in one transverse direction and iterative in the other. Helliwell and Lubard (Ref. 17), Rakich and Lubard (Ref. 18), and Line and Rubin (Ref. 16) have applied this method to flows over both sharp and spherically blunted cones at angle of attack.

In companion studies, Briley & McDonald (Ref. 19) and McDonald & Briley (Ref. 20) have developed implicit techniques for systems of coupled nonlinear equations. These techniques were applied by McDonald & Briley (Ref. 20) to the computation of laminar supersonic flow in rectangular jets. Subsequently, the laminar incompressible straight-duct analysis of Briley (Ref. 13) and the improved numerical techniques of McDonald & Briley (Ref. 20) for compressible flows were extended by Briley & McDonald (Ref. 21) and Eiseman, McDonald, and Briley (Ref. 22) into a method for computing subsonic turbulent flow in curved ducts. The present study represents a further generalization of the latter method; it encompasses general coordinates, mixed subsonic and supersonic flow, and shock waves; it is, in fact, a continuation of the study initiated by Eiseman and Levy (Ref. 23).

The basic geometry in the ogival body problem is determined by both the body itself and its bow shock. Unlike the body shape, the bow shock is not known in advance, but must be determined as part of the solution. Since the region nearest the shock is dominated by convective forces, and the shock is treated as a discontinuity, it is quite sufficient to perform a local inviscid analysis in that region; and, thereby to determine the shock location one step in advance of the fully viscous solution. The shock location is calculated numerically in terms of local extensions of the existing coordinate system. Next the shock surface is extended in a sufficiently smooth manner so that suitable coordinates can be generated for the advancement of the fully viscous solution. For this purpose, a least squares surface fitting procedure is used.

A major part of the solution procedure is the viscous approximation to the Navier-Stokes equations. Specifically, the tensor form of the Navier-Stokes equations is approximated in a coordinate independent manner to produce an initial value problem. The approximation is obtained from a neglect of viscous stresses, and hence diffusion, in an assumed primary flow direction. The approximation can be viewed as a generalization of the previous work. The primary flow direction is assumed to be given by some smooth vector field. Since the specification of any vector field is independent of coordinates, the approximation of the tensor form of the Navier-Stokes equations is also independent of coordinates. As a matter of convenience, however, the primary vector field is often chosen to be the vector field associated with a given coordinate direction of a given system of coordinates.

The final phase in the development process of a general code is the application and extension to problems of ever increasing difficulty. This phase can only be entered once the underlying structure of the general code has been established and associated coding errors have been removed. In short, a general code must be brought up to a reasonable level of development before it can be applied and extended to

cover a sequence of problems leading to a particular objective. In the case of PEPSIG the desired level of development was recently achieved. Applications and extension of the code have now been made for both internal and external flow problems. A sequence of internal flow problems has lead to successful calculations of subsonic flows in ducts with superelliptically varying cross sections under a contract with NASA Lewis Research Center. The objective for the external flow problems under the present effort was the computation of the supersonic flow over an ogival body at angle of attack. This objective involved the solution of mixed supersonic and subsonic flow; specifically, a subsonic layer is bounded by a solid object and a supersonic flow.

Before significant progress can be made on the overall program goal, the code must be able to accurately model shock waves, subsonic boundary layers, and supersonic flow with no-slip boundary conditions. Both shock waves and subsonic boundary layers have been modelled adequately and the results will be displayed along with preliminary results for supersonic flow with no-slip boundary conditions. This last case involving mixed subsonic and supersonic flow, however, has proven to be quite difficult to solve to our desired level of accuracy. Most investigators (Refs. 16-18) have noted the development of "departure solutions" as an approximate set of equations governing this mixed flow is marched in the axial direction. Suggested methods to eliminate these unwanted departure solutions have been to open up the mesh spacing to meet a certain lower bound, to specify a pressure gradient in the axial direction, and to carefully prescribe an initial profile. Although, a lower bound on the axial mesh may be required to obtain a stable marching solution of certain stiff differential equations (Ref. 24), it is disturbing when accuracy is also desired as is the case that is envisioned for the ogival body with curvature. In any case, when the axial mesh is increased for flow over a wedge, in the present cases only a decrease in the rate of growth of departure solutions is observed. The symptoms of departure solutions, however, developed immediately as indicated by the development of adverse pressure gradients in the immediate vicinity of the wall. It is also curious to note that, up to a certain point, the present solutions had many qualitatively correct features when viewed on isolated cross sections. This predicament tends to make one concerned that the previously developed remedies to suppress departure solutions are in fact, case dependent; it also points to a need for an additional general development. Recently, the problem of departure solutions has been more thoroughly investigated in Refs. 25 and 26. These investigators observed that supersonic pressure waves would propagate above the subsonic portion of the boundary layer and influence it in the upstream direction causing a pressure rise which, if left alone, would cause the solution to depart from the underlying physics. Their remedy was to specify an additional condition at the sonic line; namely, that the velocity is parallel to the wall angle. While this though proved to be more successful than that of previous investigators, when applied in the present instance, entirely satisfactory results were not obtained. In addition, two variants of this technique were tried in the present effort. Firstly, an inviscid velocity angle was specified at the sonic line

and secondly, an extrapolated angle was tried. The latter variant resulted in a slight improvement. Additional developments centered around new specifications of the axial pressure gradient in the subsonic region and on the treatment at the sonic line. To date the results, while improving, are still not satisfactory. Further work on this particular problem is obviously required.

THE GENERAL FORMATION OF AN INITIAL VALUE PROBLEM FOR STRONGLY CONVECTIVE FLOWS

Central to the present analysis is the formulation of approximate governing equations which can be solved by forward marching integration in the direction of a "primary flow". The entire flow field can thereby be obtained by a sequence of essentially two-dimensional calculations. This feature of the method results in a substantial saving of computer time and storage compared to that which would be required for solution of the full Navier-Stokes equations. The equations are derived in a coordinate independent manner. The merits of such a derivation is given in Ref. 23. A vector field that reasonably approximates the primary flow direction is chosen and then used as the basis for an approximation of the stress tensor. The time-averaged equations are written in general conservation law form, and then the approximate stress tensor is inserted to obtain the approximate equations. Note that this process depends only on the choice of a primary vector field, and not on the particular coordinate system used for the numerical solution. The primary vector field used here consists of the tangent vectors to a certain family of coordinate curves that are roughly aligned with the flow geometry.

The governing equations are derived from the Navier-Stokes equations for compressible flow of a viscous, perfect gas. In conservation law form (Refs. 27-28) and, in general curvilinear coordinates (y^1, y^2, y^3), the continuity equation is given by

$$\frac{\partial(\rho\sqrt{g})}{\partial t} + \frac{\partial}{\partial y^i}\left(\rho v^i \sqrt{g}\right) = 0 \tag{1a}$$

the momentum equations, by

$$\frac{\partial}{\partial t}\left[\rho v^i \frac{\partial x^s}{\partial y^i}\sqrt{g}\right] + \frac{\partial}{\partial y^j}\left[\left(\rho v^i v^j + \tau^{ij}\right)\frac{\partial x^s}{\partial y^i}\sqrt{g}\right] = 0 \tag{1b}$$

If constant total temperature is assumed, and energy equation is not required and can be replaced by

$$p = \rho\left[A + B g_{ij} v^i v^j\right] \tag{1c}$$

with the added assumption of a perfect gas. Otherwise, an energy equation

$$\frac{\partial}{\partial t}\left(E\sqrt{g}\right) + \frac{\partial}{\partial y^i}\left[\left\{E v^i - \varsigma^{ij} K \frac{\partial T}{\partial y^i} + g_{ri}\tau^{ij} v^r\right\}\sqrt{g}\right] = 0 \tag{1d}$$

must be used. In the above (x^1, x^2, x^3) represents fixed cartesian coordinates ρ, density; E, energy; k, thermal conductivity; A and B, constants; $\vec{V} = v^k \vec{e}_k$, velocity; $g = \det(g_{ij}) = \left|\det\left(\frac{\partial x^i}{\partial y^j}\right)\right|^2$ the metrical determinant; and τ^{ij}, the components of the stress tensor in the basis $\vec{e}_i \bullet \vec{e}_j$. In terms of the metric, the components of the stress tensor are given by

$$\tau^{ij} = g^{ij} p + \alpha_k^{ij} v^k + \beta_k^{i\ell j} \frac{\partial v^k}{\partial y^\ell} \tag{2a}$$

where

$$\alpha_k^{ij} = \mu\left(\frac{2}{3} g^{ij} \Gamma_{k\ell}^{\ell} + \frac{\partial g^{ij}}{\partial y^k}\right) \tag{2b}$$

and

$$\beta_k^{i\ell j} = \mu\left(\frac{2}{3} g^{ij} \delta_k^{\ell} - g^{i\ell} \delta_k^{j} - g^{j\ell} \delta_k^{i}\right) \tag{2c}$$

for viscosity μ, inverse metric $g^{i\ell}$, Kronecker deltas $\delta_j^i = \delta^{ij} = \delta_{ij}$, and Christoffel symbols

$$\Gamma_{ij}^k = \frac{g^{km}}{2}\left\{\frac{\partial g_{im}}{\partial y^j} + \frac{\partial g_{jm}}{\partial y^i} - \frac{\partial g_{ij}}{\partial y^m}\right\} \tag{2d}$$

In all of the above, the Einstein summation convention is assumed. That is, matching upper and lower indices are to be summed from 1 to 3 unless otherwise stated.

It is assumed that for high Reynolds number, viscous effects are negligible except in thin layers near the walls, and thus boundary layer concepts can be employed to examine relative importance of viscous terms in the governing equations. Consequently viscous terms which are considered important for boundary layer flow on walls are retained; other viscous terms are neglected. In this sense, the present approach can be regarded as a natural extension of three-dimensional boundary layer theory. Unlike conventional boundary layer theory, however, the approximate equations are to be applicable in the inviscid flow region as well as the viscous region and, thus, no approximations are made for inviscid terms other than those to be used for the pressure field in subsonic flow. A detailed account of the viscous approximation is given in Ref. 23.

METHOD OF SOLUTION

Background

The governing equations can be solved following the general approach developed in Ref. 23. The method used is based on an implicit scheme which is potentially stable for large step sizes. Thus, as a practical matter, stability restrictions which limit the axial step size relative to the transverse mesh spacing and which become prohibitive for even locally refined meshes (e.g., in laminar sublayers) are not a factor in making the calculations. The general approach is to employ an implicit difference formulation and to linearize the implicit equations by expansion about the solution at the most recent axial location. Terms in the difference equations are then grouped by coordinate direction and one of the available alternating-direction implicity (ADI) or splitting techniques is used to reduce the multidimensional difference equations to a sequence of one-dimensional equations. These linear one-dimensional difference equations can be written in block-tridiagonal or a closely related matrix form and solved efficiently and without iteration by standard block elimination techniques. The general solution procedure is quite flexible in matters of detail such as the type and order accuracy of the difference approximations and the particular scheme for splitting multidimensional difference approximations. Based on previous experience of the authors, however, it is believed that the consistent use of a formal linearization procedure, which incidentally requires the solution of coupled difference equations in most instances, is a major factor in realizing the potential favorable stability properties generally attributed to implicit difference schemes.

Numerical Techniques

As an outline of the particulars of the numerical method, the treatment of the continuity equation is considered, as this is the simplest equation, and yet this discussion will cover most aspects of the method. The flow region is discretized by grid points having spacings $\Delta x = \Delta y^3$, $\Delta y = \Delta y^1$, and $\Delta z = \Delta y^2$ respectively. Provisions for nonuniform grid spacing can be introduced as needed. The subscripts i, j and superscripts n are grid point indices associated with $y = y^1$, $z = y^2$, and $x = y^3$, respectively. Thus, $\phi^n_{i,j}$ denotes $\phi(x^n, y_i, z_j)$ where ϕ can represent any of the dependent variables. The subscripts are frequently omitted if clarity is preserved, so that ϕ^n is equivalent to $\phi^n_{i,j}$. For convenience, the following shorthand difference operator notation is used for derivative difference formulas:

$$\delta_y \phi^n = \left[\alpha\left(\phi^n_{i,j} - \phi^n_{i-1,j}\right) + (1-\alpha)\left(\phi^n_{i+1,j} - \phi^n_{i,j}\right)\right]/\Delta y \qquad (3a)$$

$$\delta_y^2 \phi^n = \left[\phi^n_{i-1,j} - 2\phi^n_{i,j} + \phi^n_{i+1,j}\right]/(\Delta y)^2 \qquad (3b)$$

with analogous definitions for δ_z, δ_z^2. Here, a parameter α has been introduced $(0 \le \alpha \le 1)$ so as to permit continuous variation from backward to forward differences. The standard central difference formula is recovered for $\alpha = 1/2$. Throughout the following discussion, it is assumed that the solution is known at x^n and is desired at x^{n+1}.

Consider the laminar continuity equation with $v^3 = u, v^1 = v, v^2 = \omega$

$$\frac{\partial}{\partial x}(\rho u J) + \frac{\partial}{\partial y}(\rho v J) + \frac{\partial}{\partial z}(\rho \omega J) = 0 \tag{4}$$

where $J = \sqrt{g}$. Equation (4) is differenced in the x or marching direction as follows:

$$\frac{(\rho u)^{n+1} - (\rho u)^n}{\Delta x} J^{n+\tilde{\beta}} + \left(\rho u \frac{\partial J}{\partial x}\right)^{n+\tilde{\beta}} + \left[\frac{\partial}{\partial y}(\rho v J) + \frac{\partial}{\partial z}(\rho \omega J)\right]^{n+\tilde{\beta}} = 0 \tag{5}$$

where $$\phi^{n+\beta} \equiv \frac{\phi^{n+1} + \beta \phi^n}{1+\beta} \quad \text{and} \quad \tilde{\beta} = \frac{\beta}{1+\beta}$$

Here, a parameter β has been introduced so as to permit a variable centering of the scheme in the x direction. Equation (5) produces a backward difference formulation for $\beta = 0$ and a Crank-Nicolson formulation for $\beta = 1$. The dependent variables in Eq. (5) are linearized in the manner of Refs. (19) and (20) by expansion about the solution at x^n. Here, a first-order accurate linearization is used for the x derivative, and the result is

$$\left[\frac{\rho^n u^{n+1} + \rho^{n+1} u^n - 2\rho^n u^n}{\Delta x}\right]\left[\frac{J^{n+1} + \beta J^n}{1+\beta}\right]$$

$$+ \frac{1}{1+\beta}\left\{\left(\rho^n u^{n+1} + \rho^{n+1} u^n - \rho^n u^n\right)\left(\frac{\partial J}{\partial x}\right)^{n+1} + \beta\left(\rho u \frac{\partial J}{\partial x}\right)^n\right\} \tag{6}$$

$$+ \frac{1}{1+\beta}\left\{J^{n+1}\delta_y\left(\rho^n v^{n+1} + \rho^{n+1} v^n - \rho^n v^n\right) + \left(\frac{\partial J}{\partial x}\right)^{n+1}\left(\rho^n v^{n+1} - \rho^{n+1} v^n - \rho^n v^n\right)\right.$$

$$\left. + \beta\left[J\delta_y\left(\rho^n v^n\right) + \left(\frac{\partial J}{\partial y}\right)^n \rho^n v^n\right]\right\}$$

$$+ \frac{1}{1+\beta}\; J^{n+1}\delta_z\left(\rho^n \omega^{n+1} + \rho^{n+1}\omega^n - \rho^n\omega^n\right) + \left(\frac{\partial J}{\partial y}\right)^{n+1}\left(\rho^n\omega^{n+1} - \rho^{n+1}\omega^n - \rho^n\omega^n\right)$$

$$\left. + \beta\left[J\delta_z\left(\rho^n\omega^n\right) + \left(\frac{\partial J}{\partial z}\right)^n \rho^n\omega^n\right]\right\} = 0$$

Neglecting for the moment the turbulent Reynolds stresses, and eliminating the pressure gradients via the equation of state, the procedure outlined above for the continuity equation can be employed to derive linear implicit difference approximations analogous to Eq. (6) for the three momentum equations. Furthermore, the resulting difference approximations can be grouped by coordinate direction and written in the following compact linear matrix difference operator notation as

$$\frac{A}{\Delta x}\left(\Phi^{n+1} - \Phi^n\right) = D_y\Phi^{n+1} + D_z\Phi^{n+1} + S \tag{7}$$

where ϕ is a column vector containing the dependent variables ρ, u, v, ω, and A is a square (4x4) matrix. D_y and D_z are 4x4 matrices containing elements which are themselves spatial difference operators for the y and z directions, respectively. S is a column vector reserved for any source terms which may be present. The matrices A, D_y, and D_z contain only quantities which are known from a computational viewpoint. Equation (7) is linear in ϕ^{n+1}.

The advantage in grouping the dependent variables by the direction of differencing is that numerous ADI or splitting techniques are immediately available for reducing the multidimensional implicit equation (13) to a sequence of one-dimensional equations (e.g., Douglas & Gunn, Ref. 29; Yanenko, Ref. 30), and this permits efficient solution while retaining the favorable stability properties of the basic implicit scheme. In previous applications of the basic numerical method used here, the Douglas-Gunn (Ref. 29) technique has been employed, as this technique produces schemes whose intermeidate steps satisfy the consistency condition and which therefore are valid for asymptotically large step sizes. In the present application, however, the technique of splitting (Yanenko, Ref. 30) is being employed at least locally, as this technique seems convenient from the standpoint of introducing approximations for the pressure field in subsonic or mixed subsonic-supersonic flow. Using the technique of splitting, Eq. (7) can be written as the following two-step scheme

$$\frac{A}{\Delta x}\left(\Phi^{*}-\Phi^{n}\right)=D_{y}\Phi^{*}+S_{1} \tag{8a}$$

$$\frac{A}{\Delta x}\left(\Phi^{n+1}-\Phi^{*}\right)=D_{y}\Phi^{n+1}+S_{2} \tag{8b}$$

where Φ^{*} is an intermediate result having computational significance but no particular physical significance, and where $S_1 + S_2 = S$.

The axial pressure gradient at the sonic line can be determined at the sonic line by extrapolation since the Navier-Stokes equations exhibit a nearly hyperbolic behavior in the sonic and supersonic regions. Similarly, the sonic line velocity can be extrapolated from nonelliptic regions. In the subsonic portion of the boundary layer the axial pressur gradient on a relatively flat surface is constant across the subsonic region. On curved surfaces, the curvature must be considered. In any case, the specification of axial pressure gradient is determined from the extrapolated gradient at the sonic line. The pressure gradients can be specified by either a direct specification by overwriting the normal momentum equation or a substitution into the normal momentum equation. These ideas are based upon the experience of previous investigators (Refs. 16-18, 25-26).

There is some arbitrariness inherent in the splitting methods concerning the source terms such as the specification of pressure gradients in subsonic regions. Computationally, this matter is nontrivial and will require further study. The procedure outlined above is not the only possible means for introducing approximations for the pressure field in the subsonic region, Indeed, the particular treatment described here is regarded as preliminary and is designed to permit an assessment of the overall approach. Further study will undoubtedly be required to establish a fully satisfactory technique for approximating and correcting the pressure field.

Solution of the Split Difference Equations

The coupled set of linear implicit difference equations arising along rows of grid points during each step of the ADI solution procedure, together with the prescribed boundary conditions, can be written in a form having the matrix structure given by a modified block tridiagonal form. Neglecting, for the moment, the modifications that resulted from boundary conditions, a direct solution by standard block elimination techniques (cf., Isaacson & Keller, Ref. 31) is both straightforward and efficient. The precise scheme used here consisted of Gaussian elimination for a simple tridiagonal system (sometimes called the Thomas algorithm) but with elements of the tridiagonal matrix treated as square submatrices rather than as simple coefficients. The required inverses of diagonal submatrices were obtained by a Gauss-Jordan reduction. The additional operations necessary to include the nonblock-tridiagonal elements are easily incorporated provided the original block tridiagonal coding is carefully organized.

THE COORDINATE SYSTEM

The Construction of Tube-like Coordinates

Tube-like coordinates will be constructed in general to provide a natural setting for the study of flows within, between, or outside of a set of prescribed tubes. The prescribed boundary tubes then become coordinate surfaces, and, as a result, the specification of fluid dynamic boundary conditions is greatly simplified. Although the equations of motion contain more terms than for a cartesian system, this does not add excessively to the run time of a program. In addition, there must be some control over the resolution of regions near bounding tubes so that the effects of wall curvature and the growth of attached boundary layers can be adequately treated. Such controls are obtained from the specification of coordinate distribution functions which shall appear only as parameters in the basic geometric construction of the coordinates. The basic geometry of the bounding tubes then provides the intrinsic constraints upon the coordinate construction. Since the primary goal is the computation of fluid flows within nontrivial geometries and not the development of coordinate systems per se, the coordinates will be kept as simple as possible, given the desired generality.

Considering various past successes of two-dimensional conformal mappings to obtain coordinates, one might naturally wish to obtain similar transformations for three-dimensions. Unfortunately, there is no three-dimensional theory of conformal transformations analogous to complex variables, and consequently, in three dimensions one is left with a complicated system of partial differential equations which generally would require numerical solution. To circumvent the considerable computational labor required for solution of such equations, a constructive process is used for the development of tube-like coordinates.

The first step in the construction of tube-like coordinates is to create a suitable family of two-dimensional surfaces which, in some sense, are transverse to a given centerline. If orthogonal coordinates are desired, then these surfaces would have to bend and flex as the tube would undergo changes in cross section at different centerline positions. In addition to the problem of constructing transverse surfaces which bend and flex, there is also the problem of constructing an orthogonal grid on a surface which has variations in Gaussian curvature, and hence, is not flat. This second problem, in fact, requires a more complicated construction than the first which in itself is not easy. Thus, the sheer magnitude of the work involved in the construction of orthogonal coordinates certainly would remove the desire for their use in fluid dynamic problems which undoubtedly would require less computation in nonorthogonal coordinates than in the construction of an orthogonal system alone. By contrast, if the transverse surfaces are selected to be two-dimensional planes, then the construction of coordinates is greatly simplified while the fluid dynamic computation is only marginally different due to coordinate nonorthogonality. Consequently the coordinate system that we shall construct will have planar transverse surfaces.

Since each planar transverse surface is a linear subspace of the real three-dimensional Euclidian vector space R^3, any such plane can be completely specified by any two spanning linearly independent vectors in R^3. The specification of the planar family of transverse surfaces is then a result of a construction of two vector fields along a given centerline curve in R^3. The origin of each plane is chosen to coincide with the associated centerline point. (See Fig. 2.) To assure that the planes are always indeed transverse, it will be assumed that they are orthogonal to the centerline at their origins. Ultimately, tube-like surfaces will be generated by loops about the planar origins which deform in some way as we move along the centerline curve; in general, these tube-like surfaces will not intersect the transverse planes orthogonally. Thus, only the centerline direction determines the transverse nature of the cross sectional planes. Specifically, the centerline tangent vectors form a vector field which, at each point, is orthogonal to the plane of the two transverse vectors, and thus each centerline point carries a triple of linearly independent vectors. By the Gram-Schmidt orthogonalization procedure, each such triple of vectors can be made into an orthogonal set, and hence, an orthonormal set which is simply called a frame. Thus, tube-like coordinate systems are constructed from a specified centerline curve and an associated frame field. Now the basic question is whether there is a canonical construction of tube-like coordinate systems from either a given centerline or a given frame field. From the theory of space curves (Ref. 32), it is well known that for positive curvature and specified torsion there is a local one-to-one correspondence between frame fields and space curves which pass through a given point. Thus, for nonzero curvature, the centerline space curve has a canonical frame field which is known as the Frenet frame. Consequently, the coordinates will be derived from the Frenet frame when it exists. At centerline points of zero curvature, the Frenet frame is degenerate and must be treated specially.

Once the Frenet frame of the space curve $\vec{\gamma}$ has been established, the unit normal and binormal vectors $\vec{V}_2$ and $\vec{V}_3$ at each point of $\vec{\gamma}$ determine a transverse plane orthogonal to the unit tangent vector $\vec{V}_1$. (See Fig. 3.) Relative to any such transverse plane, these vectors are also the standard orthonormal basis. Consequently, we can examine the plane separately from the curve, $\vec{\gamma}$, which will only appear as the point at the origin. In two dimensional functional terminology, the unit normal direction can be considered as the abscissa and the unit binormal as the ordinate; or more simply, as x and y axes, respectively. Since the tube-like coordinates are to be generated from some family of tubes encasing the space curve, $\vec{\gamma}$, a cross-sectional cut by a transverse plane produces within the plane a family of loops about the origin. We shall assume that each loop is representable by a strictly monotone radial function of angle. In this regard, a polar type of description is the most suitable. But, of course, the loops are usually more complicated than circles, and thus, we must replace the radius by a function L of both radial and angular variables r and θ. Furthermore, when noncircular loops bound a cross section of fluid, there are regions of varying wall curvature. In a numerical solution, it is desirable to put proportionately more mesh points in regions of higher curvature than in regions of less curvature. Consequently, an angular

distribution function, Θ, is a good replacement for the simple angular specification, θ, of simple polar coordinates. The net result is a generalization where polar coordinates are replaced by a pseudo-radius, r and pseudo-angle, θ. Since the loops generally vary from transverse plane to transverse plane, the pseudo-radii and angles must also be functions of axial location, t, on the centerline space curve, $\vec{\gamma}(t)$. Since the normal and binormal directions are usually functions only of the centerline curve, $\vec{\gamma}(t)$, our loops may have symmetries that do not reflect about either of these Frenet directions. Since the use of known symmetries is a great simplification in most problems, we need an option which allows one to define axes that can be aligned in an optimal way. This option is easily established from the specification of a function, $\Omega(t)$, which is a rigid rotation relative to the normal-binormal directions. To bring this development of tube-like coordinates within the framework of the preceding tensor derivations, we shall use the notation, $y^1=\theta$, $y^2=r$ and $y^3=t$ for pseudo-angular, pseudo-radial, and axial variables. In this notation, we have thus far developed (1) a length factor, $L=L(y^1, y^2, y^3)$, which is a generalization of radius, (2) an angular distribution function, $\Theta=\Theta(y^1, y^3)$ which is a generalization of angle, (3) a rotation function, $\Omega=\Omega(y^3)$, and (4) the Frenet frame, $(\vec{V}_1, \vec{V}_2, \vec{V}_3)=(\vec{V}_1(y^3), \vec{V}_2(y^3), \vec{V}_3(y^3))$ upon which the coordinates are built. That the length factor, L, and the angular distribution function, Θ, give us a generalization of polar coordinates is obvious since polar coordinates are easily retrieved by taking $L(y^1, y^2, y^3) = y^2$ and $\Theta(y^1, y^3) = y^1$. It is also worth noting that the angular distribution function, Θ, was chosen to be independent of pseudo-radius, y^2. Although it is not immediately evident, we have removed a considerable amount of potential computational complexity in the process of obtaining metric information by limiting the number of derivatives which must be computed. Furthermore, there is no real loss of flexibility in the construction of angular distribution functions. Since most commonly used analytic descriptions of loops are, in fact, controlled by a collection of parameters which depend only on axial location, y^3, a knowledge of only these parameters is often sufficient for the construction of the angular distribution function. For example, if the loops were to consist of a family of concentric homogeneous ellipses, then the major and minor axes of the outermost ellipse would form a collection of two such parameters.

With the above functions and the Frenet frame, the class of tube-like coordinates comes directly out of the transformation

$$\vec{x}=\vec{\gamma}+L\left\{\vec{V}_2 \cos\phi+\vec{V}_3 \sin\phi\right\} \tag{9}$$

which transforms curvilinear coordinates, $\vec{y} = (y^1, y^2, y^3)$ into cartesian coordinates $\vec{x} = (x^1, x^2, x^3)$ where

$$\phi(y^1,y^3)=\Theta(y^1,y^3)+\Omega(y^3) \tag{10}$$

At each transverse location, y^3, the space curve vector, $\vec{\gamma}$, translates the origin to the space curve. At a given pseudo-angle, y^1, a unit vector, $\vec{V}_2 \cos\varphi + \vec{V}_3 \sin\varphi$, is determined by the sum, $\varphi = \Theta + \Omega$ of the radial distribution function, Θ, and the transverse rotation, Ω. This unit vector sweeps out a full 360 degs in the transverse plane as y^1 passes through all of its values. Hence, we could call this a direction pointer for the transverse plane. When this direction pointer is scaled by the length factor, L, we obtain a point of our transformation. Since the length factor depends on all three variables, any set of tube-like surfaces can be obtained provided, of course, that loops are representable by a strictly monotone radial function of angle and also that no two transverse cross sections are allowed to intersect.

In a geometric setting, the transformation is really an embedding of tube-like coordinate systems into three dimensional Euclidian space. An illustration is provided in Fig. 3. From the transformation, it is also easy to see that the surfaces of constant y^3 are the transverse planes, the surfaces of constant pseudo-angle, y^1, are ruled surfaces generated from the centerline curve, $\vec{\gamma}$, and the surfaces of constant pseudo-radius, y^2, are just the concentric tubes about the space curve, $\vec{\gamma}$. Separate illustrations of these various coordinate surfaces are given in Figs. 4a, 4b, and 4c, respectively. The metric data for this transformation is given in Ref. 23.

The Length Factor

Within the structure of tube-like coordinates, the length factor contains the information needed both for the specification of basic geometry and for the distributional control of the flow region. The distributional control can be easily implemented by the use of pseudo-radial and angular distributions as merely parameters in the construction of the length factor. In this way, the basic geometry can be treated separately from the distributional aspects. The point of separation becomes especially evident when the process of length factor construction is broken down into a number of stages. Since the bounding tubes can be smoothly generated from bounding loops within each transverse plane, it is sufficient to temporarily restrict our analysis to a consideration of regions between bounding loops within a transverse plane. For our tube-like coordinates, we have implicity assumed that the nondegenerate bounding loops do not pass through the origin and are contractable along radial lines emanating from the origin. Thus, we do not allow bounding loops to intersect a radial line more than once. Consequently, each bounding loop γ_i can be expressed in terms of polar coordinates (r,θ) as the product of a single valued radial function $F_i(\theta)$ and the unit vector $(\cos\theta, \sin\theta)$. With this polar description the contraction process effectively reduces to a one-dimensional process. Specifically it is a process between the coefficients of the unit vector $(\cos\theta, \sin\theta)$. For a given set of loops $\gamma_1,\ldots,\gamma_k$ any sufficiently smooth interpolation process between the coefficients will be satisfactory. If we assume that no two tubes join within the flow region, then the flow region is divisible into subregions with no more than two bounding tubes. The interpolation process for two bounding loops γ_1, and γ_2 is, therefore, all that is usually needed; and is given by the simple homotopy

$$H(\theta,r)=L(\theta,r)(\cos\theta,\sin\theta) \tag{11a}$$

with length factor

$$L(\theta,r)=rF_1(\theta)+(1-r)F_2(\theta) \tag{11b}$$

which takes $\gamma_2(\theta) = H(\theta,o)$ uniformly and smoothly into $\gamma_1(\theta) = H(\theta,1)$ as r goes from 0 to 1. (See Ref. 33.). This is illustrated in Fig. 5. If the loop γ_2 is degenerate then the coefficient $F_2(\theta)$ vanishes and the length factor reduces to $L(\theta,r) = rF_1(\theta)$, we thus have the cross section of a duct generated by one loop. By the continuity of L as a function of γ_2, the duct generated by one loop γ_1 can be considered as a limit of annular type regions between loops γ_2 and γ_1 and γ_2 closes tightly upon the origin. This concept is often quite useful since the origin in coordinates generated from one loop suffer from the same singularity problem that occurs with simple polar coordinates. This singularity can be circumvented, however, by using an auxillary loop γ_2 which is near enough to the origin to create a good approximation to the original region. To preserve overall accuracy in a numerical computation, $||\gamma_2|| = \max_\theta F_2(\theta)$ must be less than the numerical truncation error. In fact, the well-defined limiting process would lead one to believe that there would be no problem at all in taking $||\gamma_2||$ arbitrarily small. But if $||\gamma_2||$ is taken within the region of machine roundoff error, then the singularity problem may reappear by default. Consequently, it is best to choose $||\gamma_2||$ to be much less than truncation errors but greater than roundoff errors.

The final stage of length factor construction is accomplished by a replacement of the polar coordinates r and θ by radial and angular distribution functions $R(r,t)$ and $\Theta(\theta,t)$ for axial location t. Now since R and Θ are to be the actual polar locations of a loop we must reinterpret r and θ as pseudo-radial and pseudo-angular locations on the same loop. Within this context the two-tube length factor becomes

$$L(\theta,r,t)=R(r,t)F_1(\Theta(\theta,t))+\left[1-R(r,t)\right]F_2(\Theta(\theta,t)) \tag{12}$$

and the associated unit vector becomes

$$(\cos(\Theta(\theta,t)+\Omega(t)),\ \sin(\Theta(\theta,t)+\Omega(t)) \tag{13}$$

where the rotation $\Omega(t)$ of the Frenet frame has been included for completeness.

The Construction of Bounding Tubes

As the reader has just seen, the construction of tube-like coordinate systems relies upon the existence of smooth bounding tubes. When such tubes exist at the outset of a problem, the generation of coordinates is a straightforward application of the development above. However, if the bounding tubes are unknown at the outset, then they must be constructed in a smooth enough fashion. In such cases one is often given a discrete specification of a sequence of bounding loops which first must be fit with a smooth curve and then must be joined to form a smooth surface. This circumstance can often arise out of the convenience associated with the discrete specification of a surface by means of successive cross sectional cuts. If this data were to be given all in advance of the intended use of the coordinate system as a whole, then the smoothed cross sectional loops could be effectively joined by fitting them together with splines which can have interior knots corresponding to interior loops. However, it is often the case that discrete loop data is only generated one station in advance of the use of the coordinate system. This occurs, for example, when the problem is to solve for the viscous flow field outside of an ogival body when the flow is predominately supersonic. While the ogival body surface is known in advance, the location of the bow shock is not. Thus one considers the ogival body surface as the unknown outer tube which one wishes to use for the generation of tube-like coordinates to allow for the efficient computation of the fully viscous flow field. Since the flow field in a neighborhood of the bow shock is largely inviscid, an inviscid explicit solution is performed iteratively to obtain discretely the geometry of the bow shock at one station in advance of our known soltuion and coordinate system. One is now left with a fully developed bow shock surface preceeded by a discrete cross sectional loop of bow shock data. The problem is to smoothly fit the loop and then smoothly join the result to obtain a smooth extension of the surface. Since fluctuations may arise from the discrete generation of the bow shock data, a least squares spline procedure is used to fit the loop with smoothness up to three continuous derivatives. This type of least-squares procedure has the distinct advantage of accurately representing the surface normal curvature along the loop. Now one has a loop $\gamma_{n+1}(\theta)$ at level n+1 and a bounding tube ending on a loop $\gamma_n(\theta)$ at level n where there are known derivatives in the axial direction t. One then attaches a surface which extends the tube from γ_n to γ_{n+1} with the smoothness of three continuous derivatives. The extension is accomplished with the tensor product form

$$p(\theta,t)=\sum_{j=0}^{r+1} f_j(t)\,\gamma_{n+1-j}(\theta) \qquad (14)$$

which takes information back to loop γ_{n-r}. At the beginning r must be 1 since there are only two available loops. The process continues with r increasing until a desired maximum r value is obtained. From there on r is assumed to be constant.

Distribution Functions

When partial differential equations are discretized in terms of differences, the derivatives are replaced in some fashion by difference quotients. A simplification then leads to the difference equations that we solve. Implicitly in the discretization, however, is the assumption that derivatives are accurately estimated by secant lines. But then the exact solution may experience drastic variations in a short distance. Such solutions are said to have large gradients. In regions where the gradients are large, the approximation of derivatives by secants may be very poor unless the particular region is disected into smaller regions which have reasonable secant approximations, a practice commonly known as mesh refinement. In fluid mechanics, the boundary layer of a viscous flow around or through an object is such a region.

Obviously, the necessary resoltuion could be accomplished by merely increasing the number of points in a uniform distribution; however, this would require excessive computer time and storage. Another alternative, known as the interface method, is to use a refined mesh only in the given region and then join it with the global mesh. An improved technique is to use coordinate distribution functions which smoothly distribute mesh points so that in some sense they are spaced in roughly an inverse proportion to the size of the gradients. Thus, regions of high gradients have proportionately more points than regions with smaller gradients. Unlike the interface method, the transition between different mesh lengths is made continuously, and as gradually as possible. Distributions are often used when the distributional transformation is applied to an independent variable of an existing transformation. The result is a new transformation obtained by composition. With this approach, the problem of mesh point distribution is replaced by the problem of selecting a suitable set of distribution functions within a transformation of coordinates. The problem is a nontrivial one since the distribution functions should depend upon the nature of the solution being computed but are determined in advance of the computation. Thus, some prior knowledge of the solution is required. In flows with large boundary layer separation or with adjacent dissimilar components, the critical region to be resolved is somewhere in the middle of the flow. But the location of such regions is often unknown at the outset of the problem. One method to overcome this difficulty in marching procedures is to create the distribution function at the next level based upon a knowledge of the solution at the present level. Care must be taken, however, to create a distribution function that is sufficiently smooth in the marching direction.

In many problems of practical interest, however, the regions that need resolution are known in advance. Typical examples are attached boundary layers and boundary layers that may have small separations or separation bubbles.

Within the framework of tube-like coordinate systems boundary layer resolution (Ref. 28) on the inner surface is accomplished by setting

$$R(r,t) = \frac{d}{\alpha} r + \left(1 - \frac{d}{\alpha}\right)\left[1 - \frac{\tanh D(1-r)}{\tanh D}\right] \qquad (15)$$

where $d = d(t)$ is the estimated boundary layer growth, $\alpha = \alpha(t)$ is the desired proportion of mesh points in the boundary layer, and D is the hyperbolic damping factor. The boundary layer growth d gives the fraction of the flow region occupied by the boundary layer, α is usually taken as a constant, and D can be given a value of about 2. When r is small, the radial distribution of equation (45) reduces essentially to the line

$$R \simeq \frac{d}{\alpha} r \qquad (16)$$

which would have been chosen had we used the interface method. As r approaches unity the distribution Eq. (15) smoothly approaches unity as illustrated in Fig. 6.

TREATMENT OF THE BOW SHOCK

Although the shape of the body is specified at the start of the problem, the shape of the bow shock cannot be specified until effects of the body on the flow within the bow shock are evaluated. The shock shape is therefore evaluated at each new marching station based on information already computed. The shock surface is adopted as the outer coordinate surface and is used to determine the necessary metric information for the tube-like coordinates. The governing equations are then solved in the annular region between the ogival body and the bow shock by marching from one transverse plane to the next, proceeding in the nominally streamwise direction.

The bow shock is computed as a discontinuity satisfying the classical Rankine-Hugoniot relations. The intersection of this shock and a transverse computational plane is a loop represented by discrete grid points. Provided that a given grid point on this loop is outside the "zone of influence" of the neighboring points on the loop, the shock solution at the given point is independent of the solution at adjacent points. This "zone of influence" assumption is valid over a wide range of flow conditions and consequently is not a limiting assumption. Thus the shock radius $\gamma_{n+1}(\theta)$ at each point in the n+1 transverse plane can be evaluated independently by a pointwise iteration procedure.

The iteration at each circumferential location in the n+1 plane proceeds by first locally extending the shock surface from the most recently evaluated transverse computational plane, n, to a point in the n+1 plane. The extension of the shock surface includes the point being evaluated in the n+1 plane, but does not extend circumferentially to the neighboring points. This extension is a first guess for the shock location at a circumferential point and hence for a point on the outer tube-like coordinate surface given by $\gamma_{n+1}(\theta)$ in Eq. (14).

Given a guess at the shock location, the axial mass flux inside the shock can be computed by two methods. First, an application of the Rankine-Hugoniot conditions produces a value of the axial mass flux based only on the shock shape and the flow properties outside the shock. Second, an application of a compatibility condition produces a second value of this flux that depends only on the shock shape and the flow properties inside the shock. The shock location is then adjusted iteratively until the axial mass flux inside the shock computed by the two methods is the same. This iteration for the shock location is repeated at each of the circumferential grid points to produce a ring of discrete points at the n+1 station which collectively determine the shock surface. These discrete points must be represented by a continuous smooth curve to provide the information required to construct the coordinate system. For this purpose a least squares-spline curve fitting routine is employed.

ACKNOWLEDGMENT

The work contained in this report was initiated while the second author, H. McDonald, was an employee at United Technologies Research Center. H. McDonald remained active in a consulting role over the last eleven months of the contract while an employee of Scientific Research Associates. His role as a consultant is gratefully acknowledged.

RESULTS

A number of test cases were run to test, evaluate, and extend the PEPSIG code on sequence of flow problems. The sequence of problems was chosen to reflect the various types of flow situations that are likely to occur in the complex flow field over an ogival body of arbitrary geometry when it is at an angle of attack. Since the flow has subsonic regions, supersonic regions, and shock waves it is imperative that test cases should be successfully executed when these flow types are isolated and when they occur simultaneously. Since purely subsonic flow has been successfully done for boundary layers and for internal duct flow under a separate project for NASA Lewis, it need not be displayed here. For purely supersonic flow with shocks, several test cases were run. First, it was desired to correctly model a shock wave and allow it to properly be passed out of the computational region. The ability to pass shock waves out of a region required the application of exit derivative conditions aligned with the shock angle. In Fig. 7 a spurious shock reflection is observed which is corrected by the development of exit derivative conditions as displayed in Fig. 8. In each case, the specified shock angle was correctly preserved as the solution was marched upstream. However, the solution in each case possessed wiggles. To remove these wiggles a fourth order damping term was added. In the present implicit procedure a modified form of the fourth-order pressure damping term suggested by MacCormack and Baldwin (Ref. 34) and modified in Ref. 35, has been employed, viz., a term of the form

$$D_{\rho_k} = \eta_k \frac{\partial^2 \phi}{\partial x_k^2} \tag{17}$$

has been added to each of the governing equations being solved for each coordinate direction x_k. The diffusion coefficient η_k in Eq. (17) was taken as

$$\eta_k = \beta (\Delta x_k)^3 f \cdot \frac{|u_k| + c}{4 \bar{p}} \left(\frac{\partial^2 p}{\partial x_k^2} \right) \tag{18}$$

where $0 < \beta \leq 1/2$, c is the local sound speed, and the average pressure $\bar{p}$ given by

$$\bar{p} = \frac{1}{4} \left(p_{i-1} + 2p_i + p_{i+1} \right) \tag{19}$$

where i is the grid point index in the x_k-direction. In the damping term the factor f is set to 1.0 for the continuity equation and to ρ for all other conservation equations. For the free shock, cross sectional results without damping in Figs. 9, and 10 are improved with damping as displayed in Figs. 11 and 12. Here, a sequence

of cross sectional cuts are given to show that the remaining post shock wiggles are dissipated into smooth curves as the solution is marched in the upstream direction. With the ability to correctly model purely subsonic flow and purely supersonic flow with shocks, it remains to demonstrate test cases with mixed subsonic and supersonic regions. The initial extension in this direction was performed on the model problem of a supersonic flow over a flat plate with no-slip boundary conditions. The no-slip boundary condition forces a subsonic region in the wall vicinity. In particular, a Mach 2 free stream flow developed a boundary layer with a subsonic region. Profiles of velocity, density, pressure, and Mach number are given in Figs. 13 to 17. Figure 13 gives calculated values of the streamwise velocity. It should be noted that although a subsonic region clearly exists in the vicinity of the wall (see Fig. 17), the calculation produced qualitatively reasonable profiles. The calculated transverse velocity, density, pressure distributions and Mach number are presented in Figs. 14-17, respectively. This calculation is an indicator of a basic capability of the code to model a supersonic flow with a no-slip boundary condition. Similarly, supersonic flow with an imbedded shock wave over a wedge was considered. Cross sectional profiles are displayed in Figs. 18 and 19. In each case above, the cross sectional profiles appear to correctly model the physics. However, in the streamwise direction, there was a gradual development of an adverse pressure gradient. This was caused by supersonic pressure waves impinging upon the subsonic portion (Refs. 25-26); the result is the development of departure solutions (Refs. 16-18, 25-26). In Issa and Lockwood (Ref. 26) the suggestion is to apply a special condition at the sonic line while the other investigators (Refs. 16-18) have tried various specifications of the subsonic axial pressure gradient. With due consideration to the results of the other investigators, a more satisfactory resolution to the problem of departure solutions is still being sought.

REFERENCES

1. Rainbird, W. J.: Turbulent Boundary Layer Growth and Separation on a Yawed 12 ½° Cone at Mach Numbers 1.8 and 4.25. AIAA Paper No. 68-98, January 1968.

2. Tracy, W. R.: Hypersonic Flow Over a Yawed Circular Cone. Mem. 69. Graduate Aeronautical Laboratories, California Institute of Technology, August 1963.

3. Stetson, K. F.: Experimental Results of Laminar Boundary Layer Separation on a Slender Cone at Angle of Attack at $M_\infty = 14.2$. ARL Report 71-0127.

4. Rainbird, W. J.: The External Flow Field About Yawed Circular Cones. AGARD Specialists Meeting, Hypersonic Boundary Layers and Flow Fields, London, May 1968.

5. Moretti, G.: Inviscid Flow Field Past a Pointed Cone at an Angle of Attack. General Applied Science Laboratory, Tech. Report 577, December 1965.

6. Moretti, G. and M. Abbett: A Time Dependent Computational Method for Blunt Body Flows. AIAA Journal, Vol. 4, No. 12, December 1966.

7. Lomax, H. and M. Inouye: Numerical Analysis of Flow Properties about Blunt Bodies Moving at Supersonic Speeds in an Equilibrium Gas. NASA TR R-204, 1964.

8. South, J. C. and E. B. Klunker: Methods for Calculating Nonlinear Conical Flows. NASA SP-228, 1969.

9. MacCormack, R. W. and R. F. Warming: Survey of Computational Methods for Three-Dimensional Inviscid Flows with Shocks. Advances in Numerical Fluid Dynamics, AGARD Lecture Series 64, Brussels, Belgium, February 1973.

10. Boerike, R. R.: The Laminar Boundary Layer on a Cone at Incidence in Supersonic Flow. AIAA Paper 70-48, January 1970.

11. Patankar, S. V. and D. B. Spalding: A Calculation Procedure for Heat, Mass, and Momentum Transfer in Three-Dimensional Parabolic Flows. Int. J. Heat and Mass Transfer, Vol. 15, 1972, p. 1787.

12. Caretto, L. S., R. M. Curr, and D. B. Spalding: Computational Methods in Applied Mechanics and Engineering, Vol. 1, 1973, p. 39.

13. Briley, W. R.: Numerical Method for Predicting Three-Dimensional Steady Viscous Flow in Ducts. Journal of Computational Physics, Vol. 14, 1974, p. 8.

REFERENCES (CONT'D)

14. Patankar, S. V., V. S. Pratap, and D. B. Spalding: Prediction of Laminar Flow and Heat Transfer in Helically Coiled Pipes. Journal of Fluid Mechanics Vol. 62, 1974, p. 539.

15. Rubin, S. G., and T. C. Lin: A Numerical Method for Three-Dimensional Viscous Flow: Application to the Hypersonic Leading Edge. Journal of Computational Physics, Vol. 9, p. 339, 1972.

16. Lin, T. C., and S. G. Rubin: Viscous Flow Over a Cone At Moderate Incidence. Part 2 Supersonic Boundary Layer. Journal of Fluid Mechanics, Vol. 59 Part 3, p. 593, 1973.

17. Helliwell, W. S., and S. C. Lubard: An Implicit Method for Three-Dimensional Viscous Flow With Application to Cones At Angle of Attack. Computers and Fluids, Vol. 3, p. 83, 1975.

18. Rakich, J. V., and S. C. Lubard: Numerical Computation of Viscous Flows on the Lee Side of Blunt Shapes Flying at Supersonic Speeds. Aerodynamic Analyses Requiring Advanced Computers. Part 1. NASA SP-347, 1975.

19. Briley, W. R. and H. McDonald: An Implicit Numerical Method for the Multidimensional Compressible Navier-Stokes Equations. United Aircraft Research Laboratories Report M911363-6, November 1973.

20. McDonald, H. and W. R. Briley: Three-Dimensional Supersonic Flow of a Viscous or Inviscid Gas. United Aircraft Research Laboratories Report N111078-1, November 1974.

21. Briley, W. R. and H. McDonald: Computation of Three-Dimensional Turbulent Subsonic Flow in Curved Passages. United Aircraft Research Laboratories Report R75-911596-8, March 1975.

22. Eiseman, P. R., H. McDonald, and W. R. Briley: A Method for Computing Three-Dimensional Viscous Diffuser Flows. United Technologies Research Center Report R75-911737-1, July 1975.

23. Eiseman, P. R. and R. Levy: A Method for Computing Three-Dimensional Viscous Flows Over an Ogival Body at Angle of Attack. United Technologies Research Center Report R76-912024-8, February 1976.

24. Curtiss, C. F. and J. O. Hirschfelder: Integration of Stiff Equations. Proceedings of the National Academy of Sciences. Vol. 38, No. 3, pp. 235-243 (1952).

25. Issa, R. I. and F. C. Lockwood: On the Prediction of Two-Dimensional Supersonic Viscous Interactions Near Walls. AIAA Journal, Vol. 15, No. 2, pp. 182-188 (1977).

26. Issa, R. I, and F. C. Lockwood: A Hybrid Marching Integration Procedure for the Prediction of Two-Dimensional Supersonic Boundary Layers. ASME Journal of Fluids Engineering, pp. 205-212, (1977).

27. Eiseman, P. R.: The Numerical Solution of the Fluid Dynamic Equations in Curvilinear Coordinates. Air Force Weapons Laboratory Technical Report AFWL-TR-73-172, August 1973.

28. Eiseman, P. R.: A Coordinate System for a Viscous Transonic Cascade Analysis. Journal of Computational Physics. To Appear.

29. Douglas, J. and J. E. Gunn: A General Formulation of Alternating Direction Methods, Part I. Parabolic and Hyperbolic Problems. Numerische Mathematik Vol. 6, p. 428, (1964).

30. Yanenko, N. N.: The Method of Fractional Steps. Translation Edited by M. Holt. Springer-Verlag, New York 1971.

31. Isaacson, E. and H. B. Keller: Analysis of Numerical Methods. John Wiley & Sons, Inc. New York (1966).

32. Laugwitz, D.: Differential and Riemannian Geometry. Academic Press, Inc. New York (1965).

33. Hu, S-T: Homotopy Theory. Academic Press, Inc., New York (1959).

34. MacCormack, R. W. and B. S. Baldwin: A Numerical Method for Solving the Navier-Stokes Equations with Application to Shock-Boundary Layer Interactions. AIAA Paper 75-1, AIAA 13th Aerospace Sciences Meeting, 1975.

35. Levy R., S. J. Shamroth, H. J. Gibeling, and H. McDonald: A Study of the Turbulent Shock Wave Boundary Layer Interaction. AFFDL-TR-76-163, February 1977.

FLOW PAST AN OGIVE AT INCIDENCE

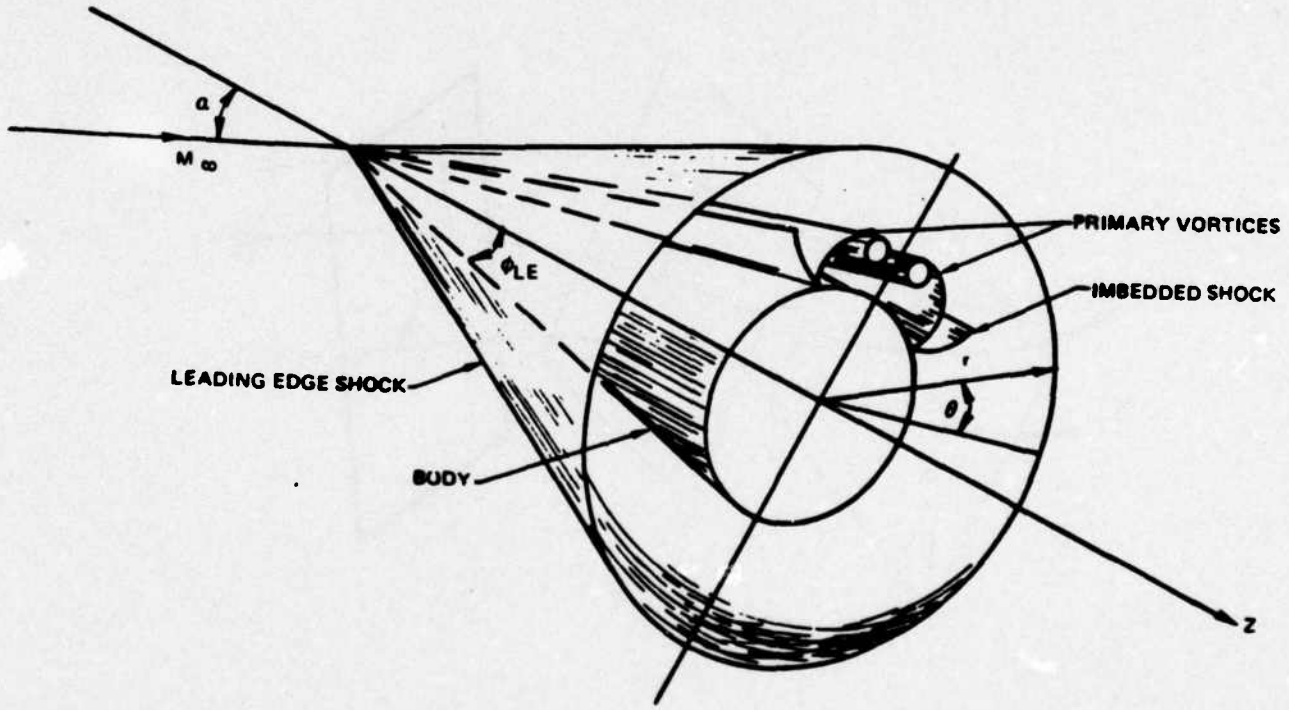

GENERATION OF TRANSVERSE PLANES FROM TWO VECTOR FIELDS

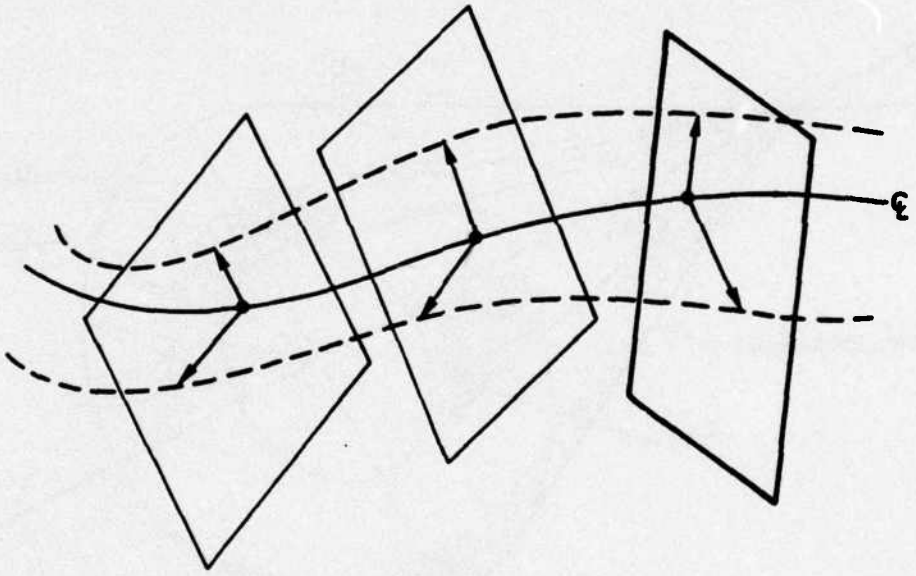

TRANSFORMATION AS AN EMBEDDING
INTO THREE DIMENSIONAL EUCLIDIAN SPACE

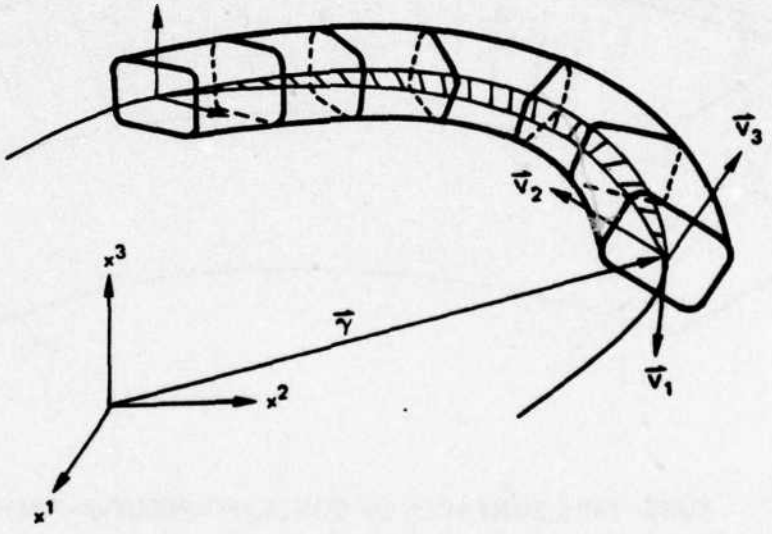

R07-84-14

FIG. 4

a TRANSVERSE PLANAR CUTS OF CONSTANT AXIAL LOCATION y^3

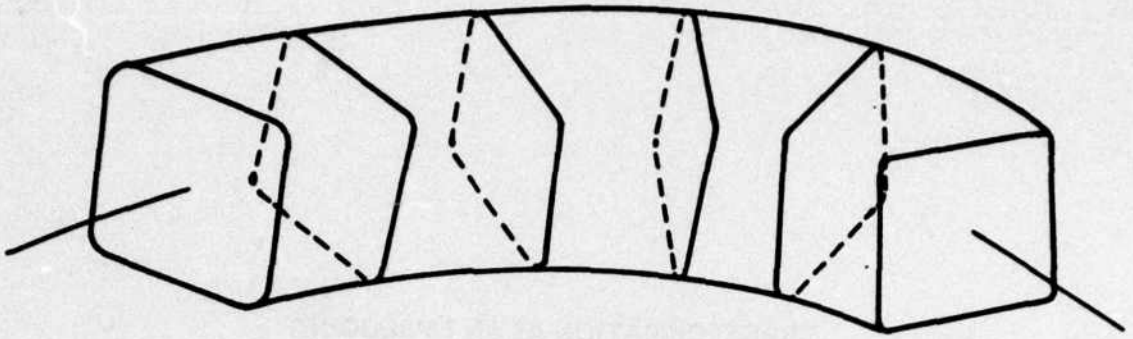

b RULED SURFACE OF CONSTANT PSEUDO-ANGLE y^1

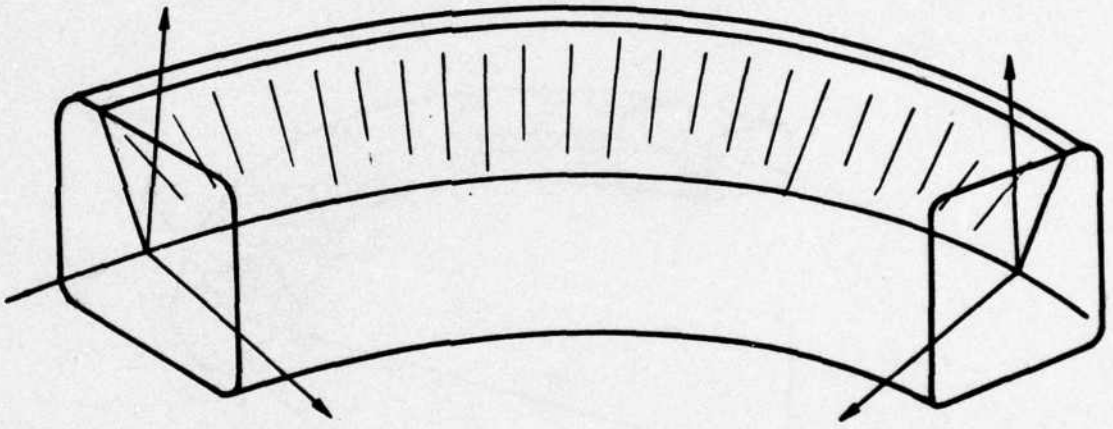

c TUBE-LIKE SURFACES OF CONSTANT PSEUDO-RADIUS y^2

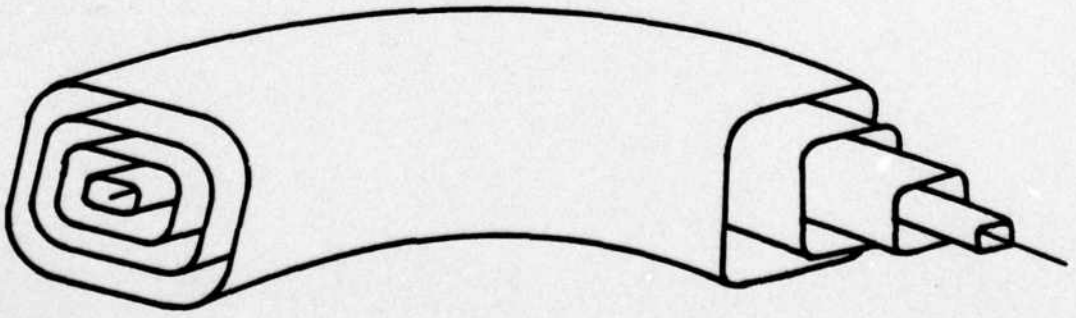

R07-84-1

LINEAR HOMOTOPY BETWEEN TWO LOOPS

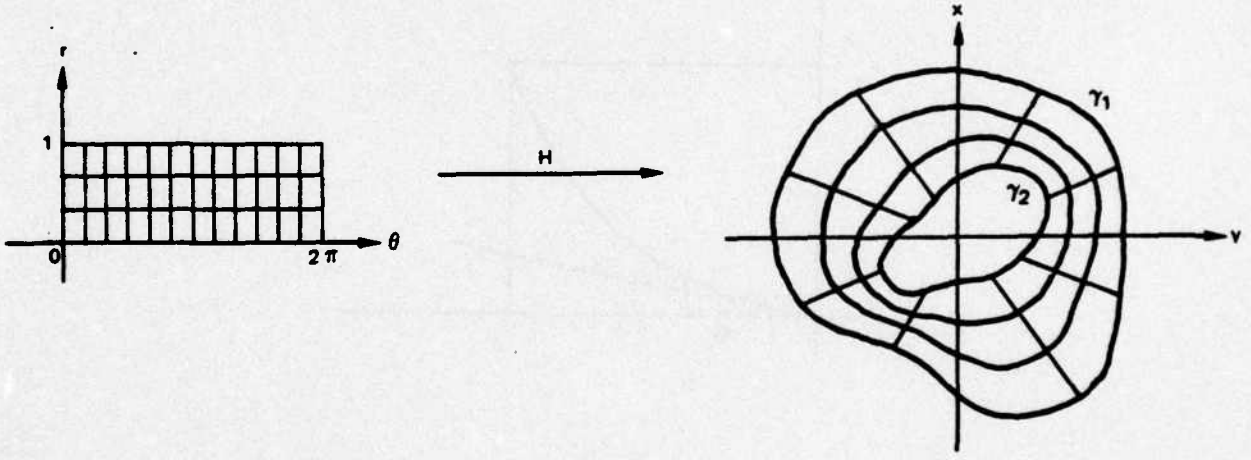

RADIAL DISTRIBUTION FUNCTION

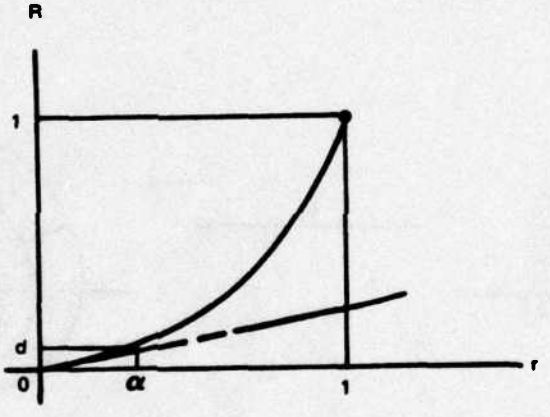

FIG. 7

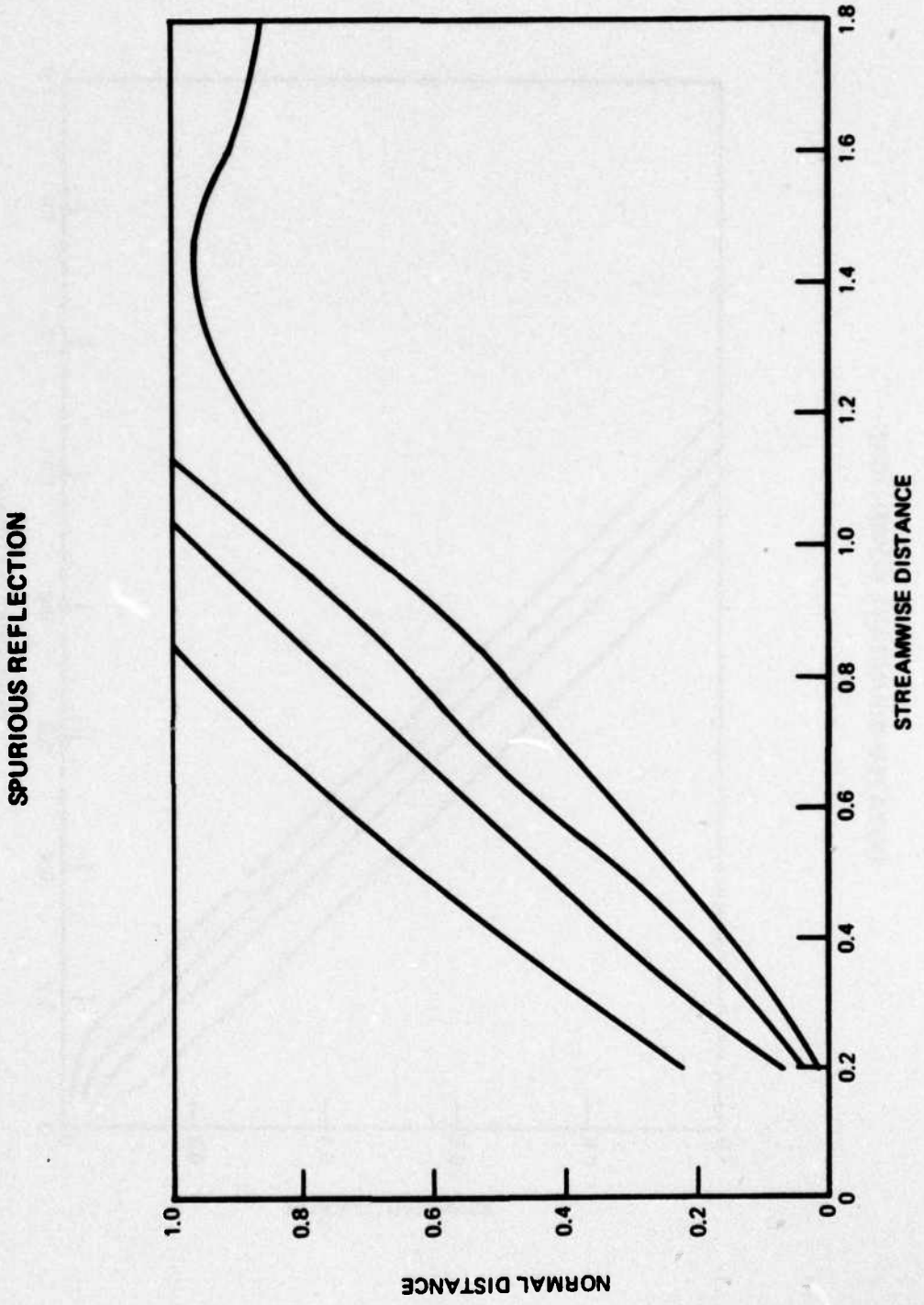

77-06-168-1

ROTATED BOUNDARY CONDITIONS

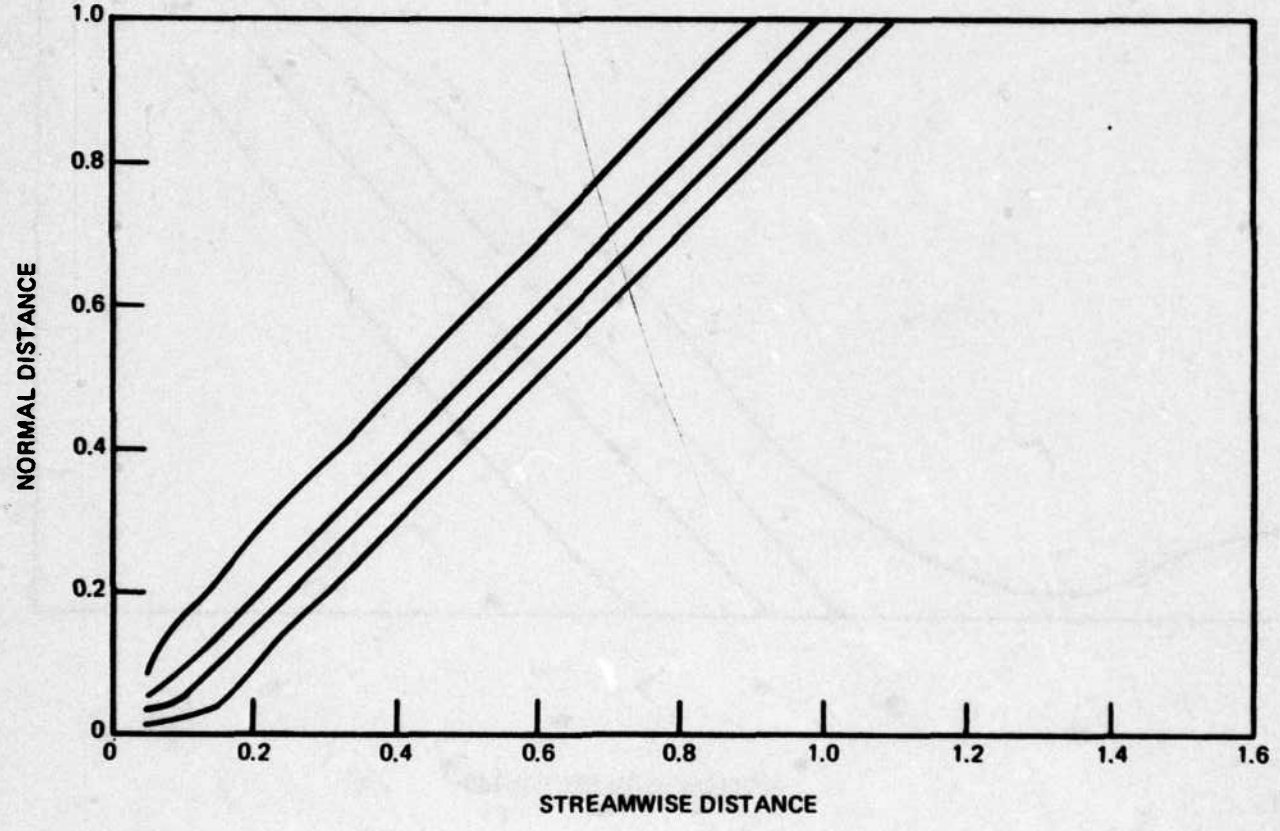

77-06-182-2

FIG. 8

FREE SHOCK WITHOUT DAMPING

NRAD = 15, ΔX = 0.2
NRAD = 15, ΔX = 0.05
NRAD = 21, ΔX = 0.05

NRAD IS THE NUMBER OF TRANSVERSE POINTS

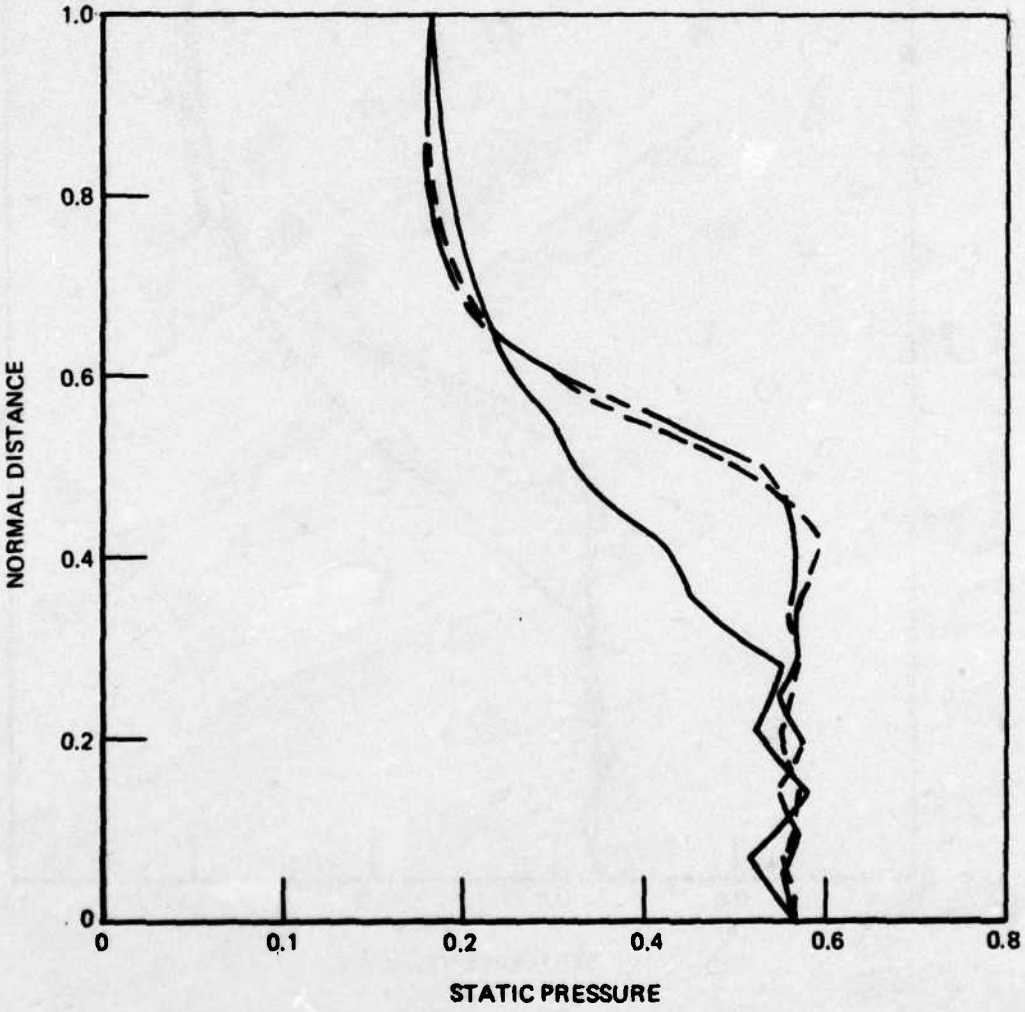

77-06-168-3

FIG. 10

FREE SHOCK WITHOUT DAMPING

NRAD = 15, ΔX = 0.2
NRAD = 15, ΔX = 0.05
NRAD = 21, ΔX = 0.05

NRAD IS THE NUMBER OF TRANSVERSE POINTS

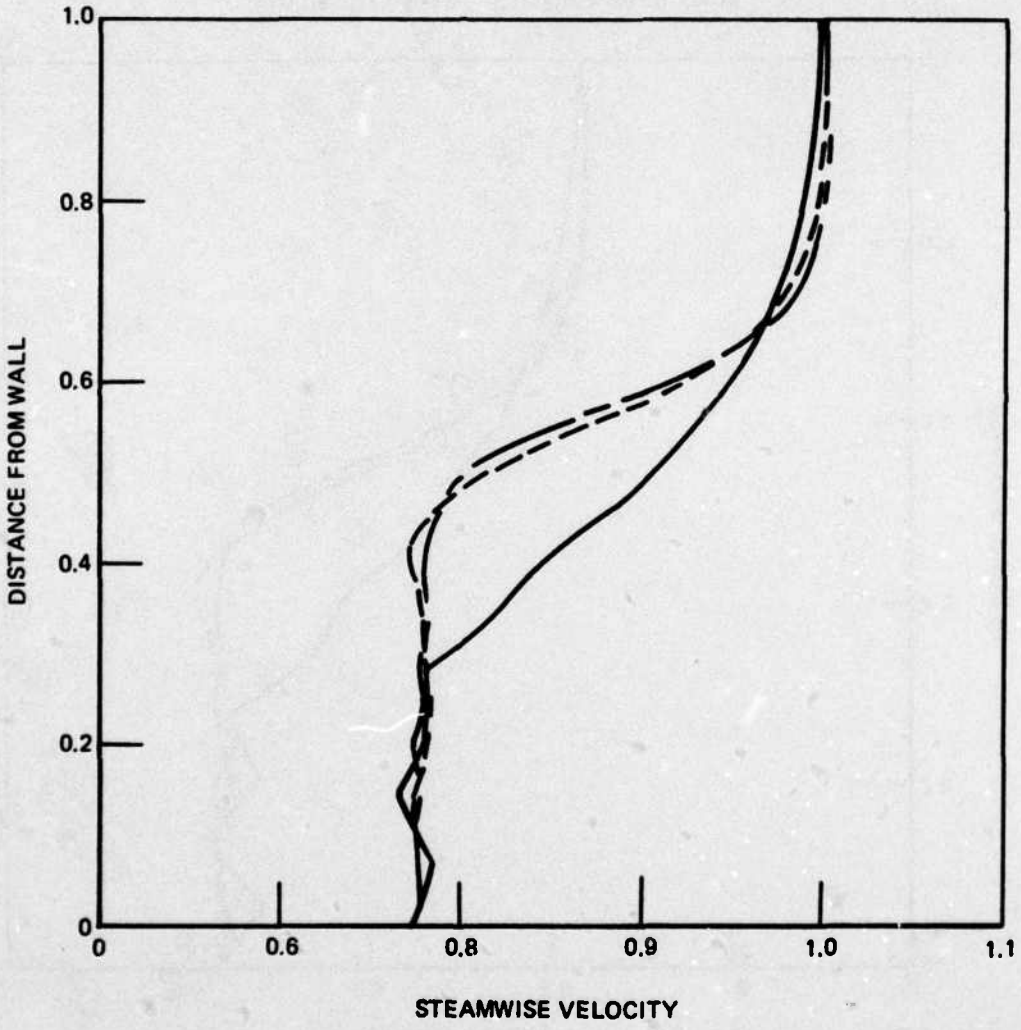

77-06-168-4

FREE SHOCK WITH DAMPING

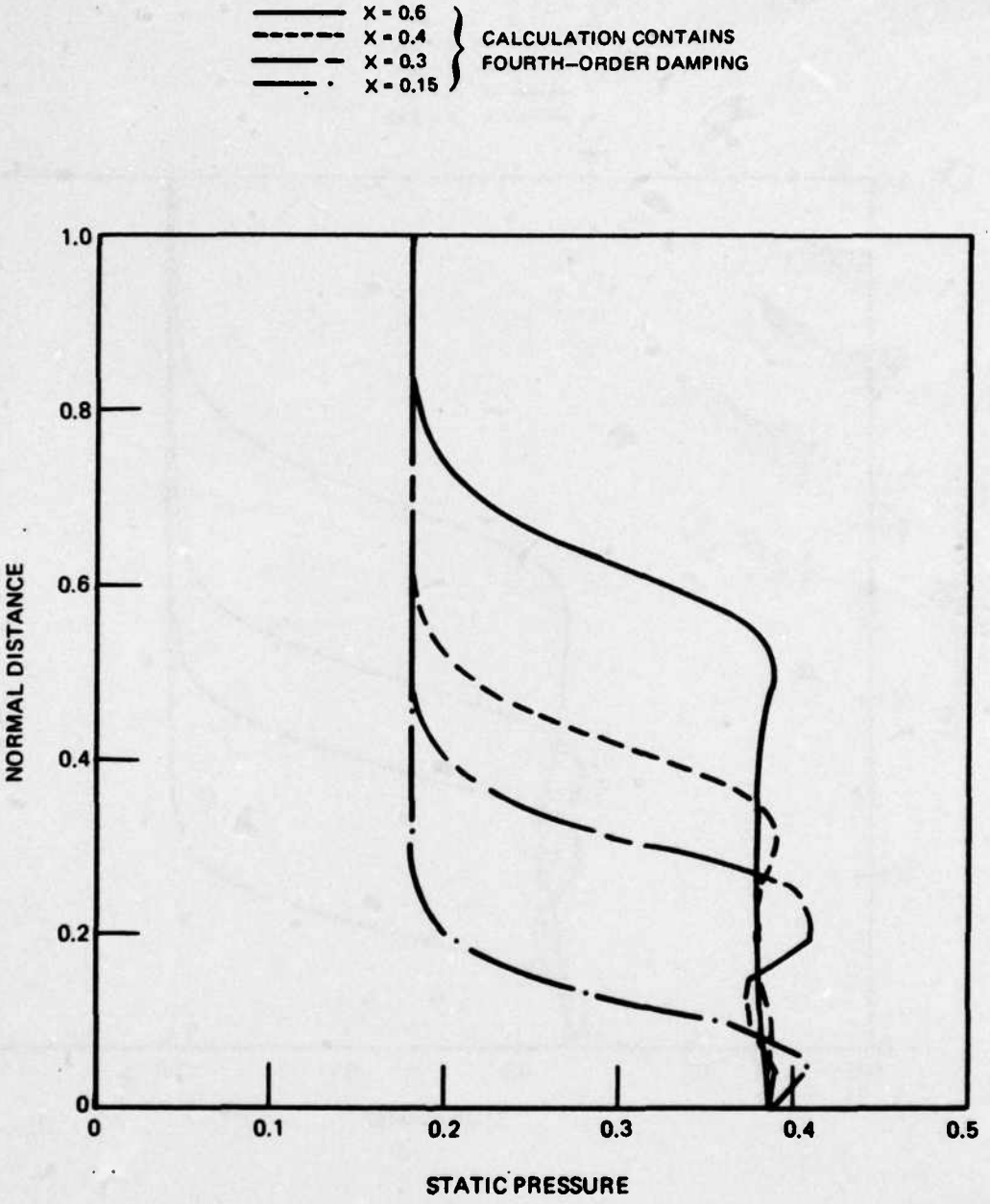

77-06-188-5

FREE SHOCK WITH DAMPING

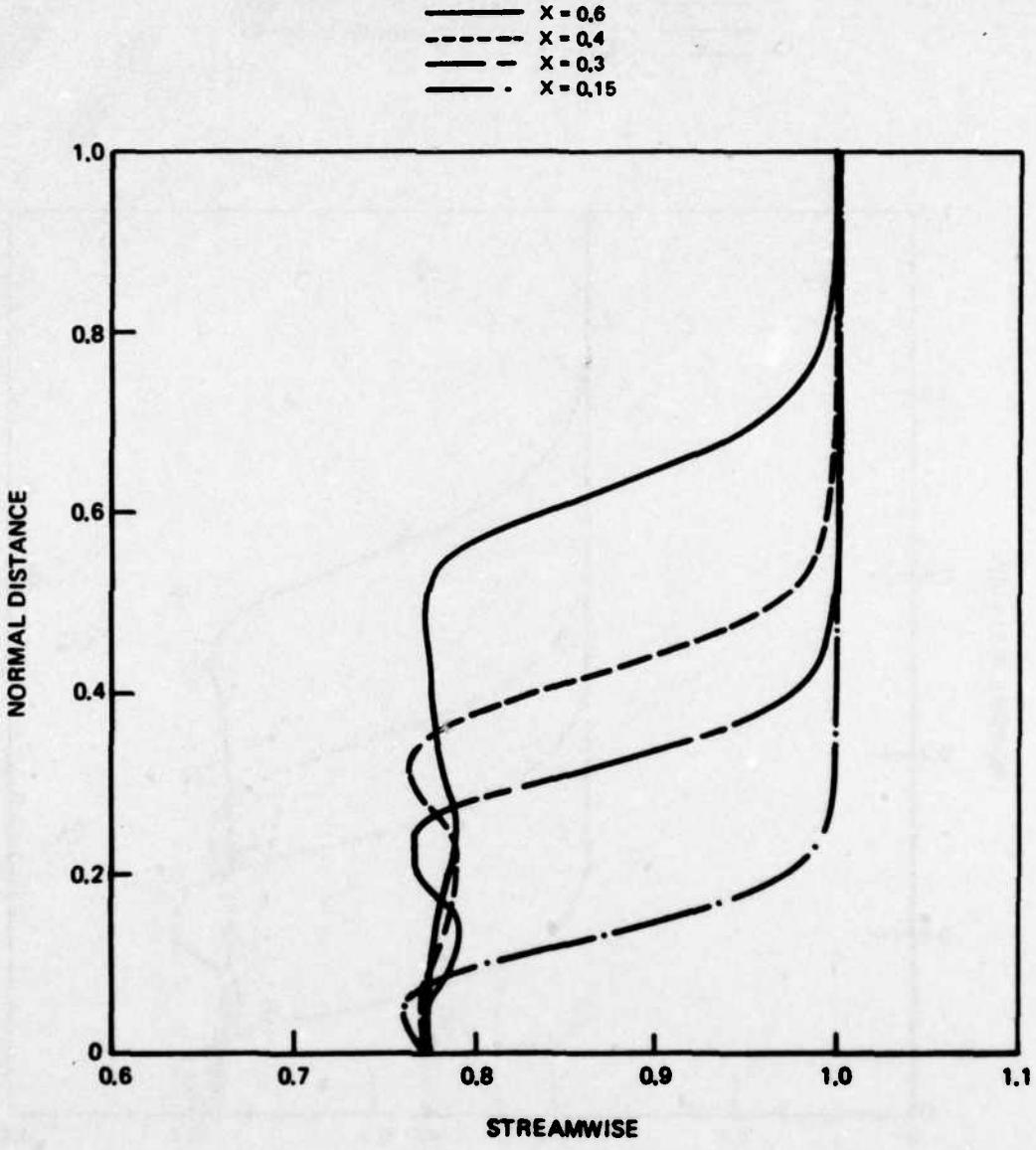

VELOCITY PROFILE FOR WEDGE

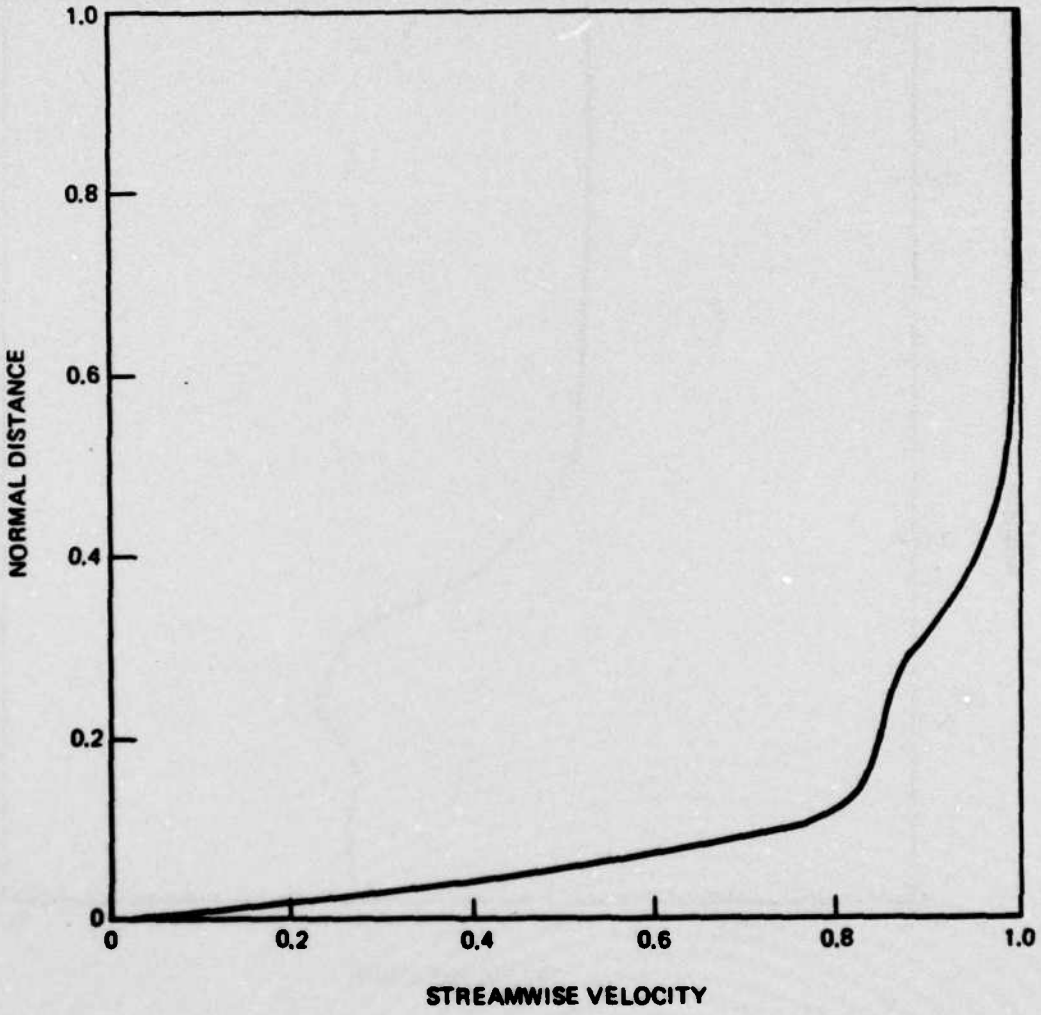

77-06-168-7

PRESSURE PROFILE FOR WEDGE

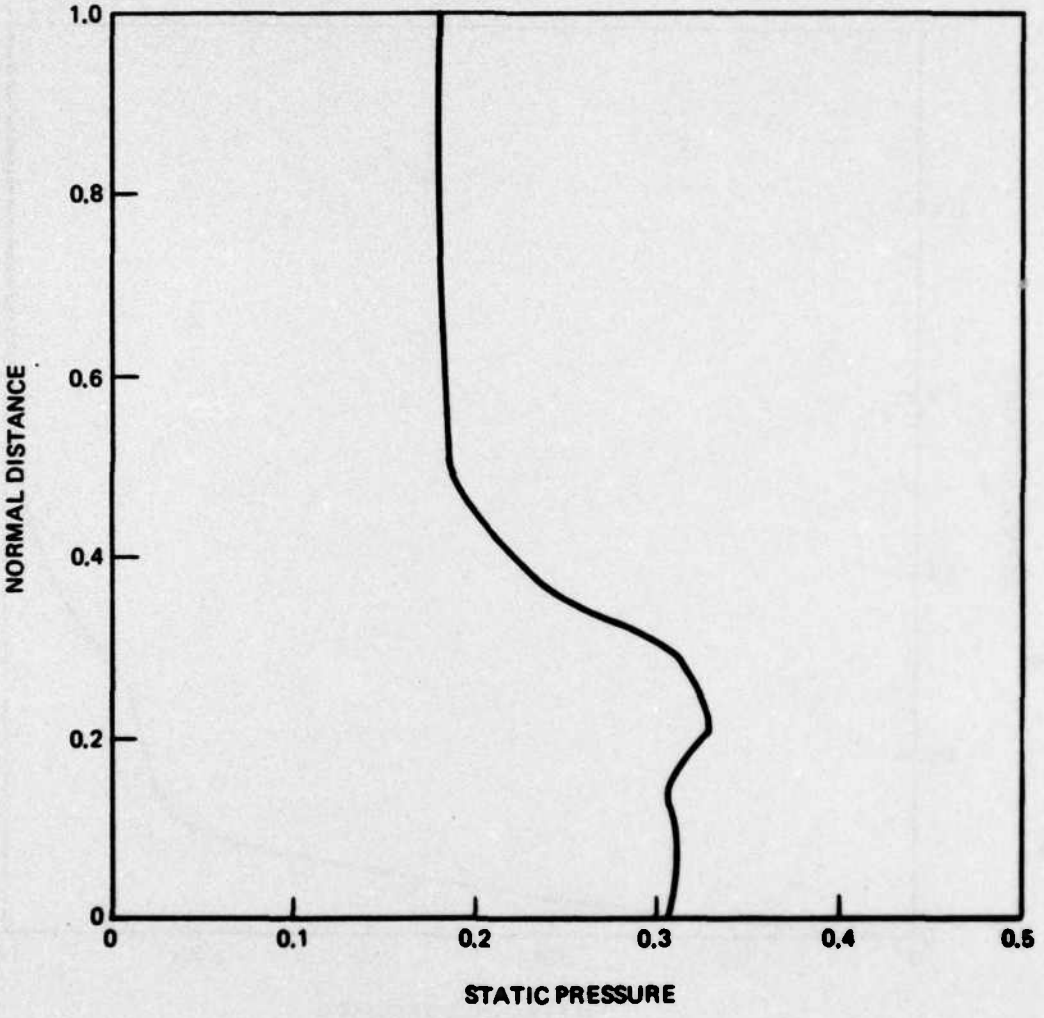

77-08-168-8

DEMONSTRATION OF SUPERSONIC FLOW CALCULATION WITH SUBSONIC WALL REGION

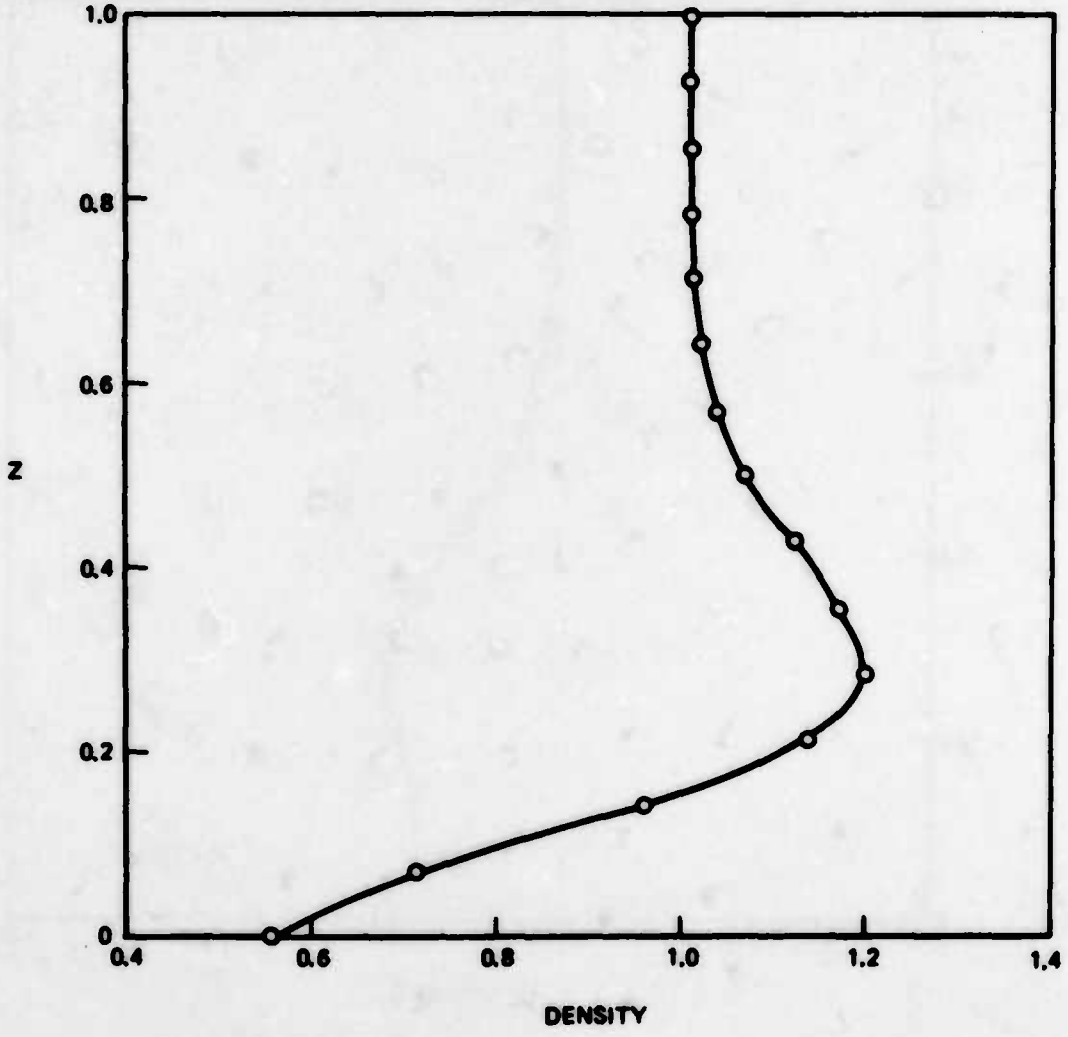

DEMONSTRATION OF SUPERSONIC FLOW CALCULATION WITH SUBSONIC WALL REGION

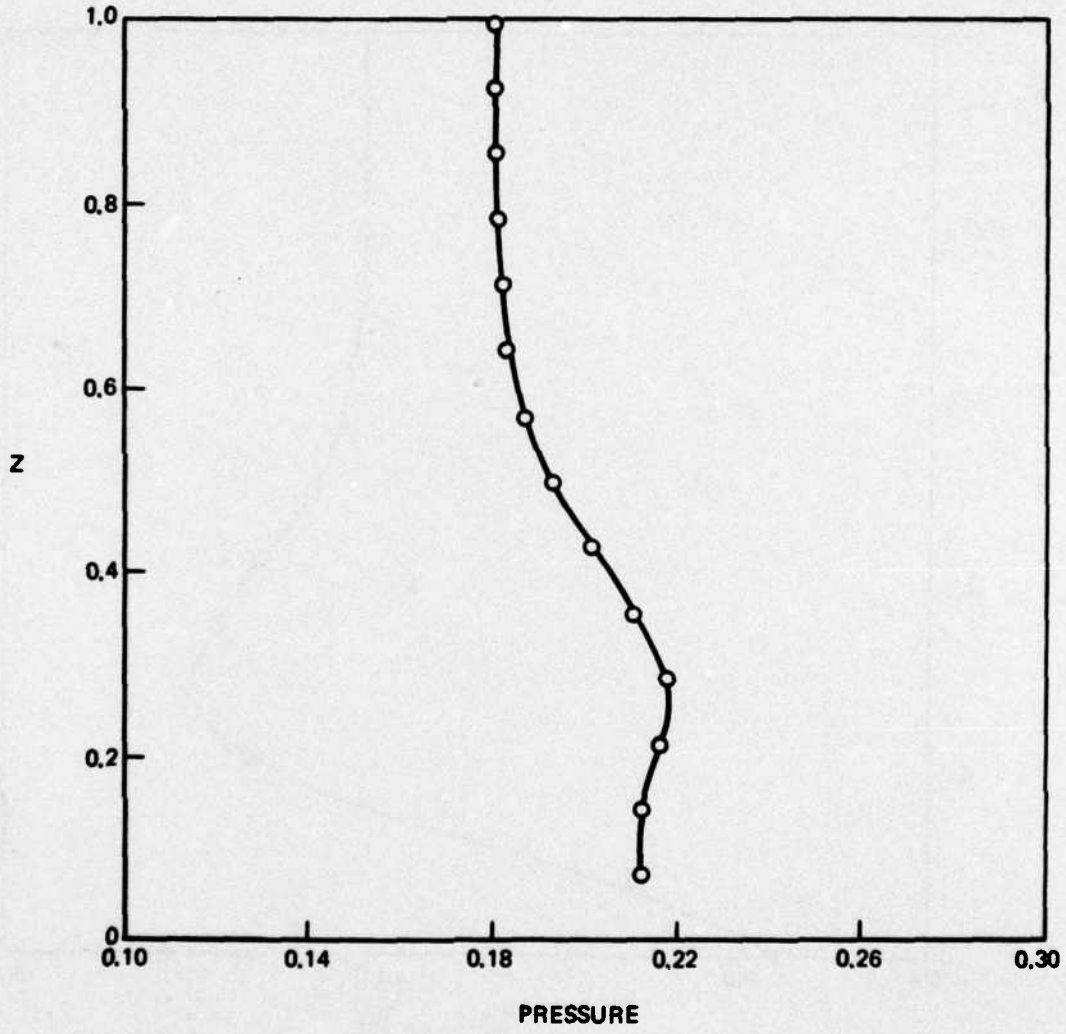

77-06-168-10

DEMONSTRATION OF SUPERSONIC FLOW CALCULATION WITH SUBSONIC WALL REGION

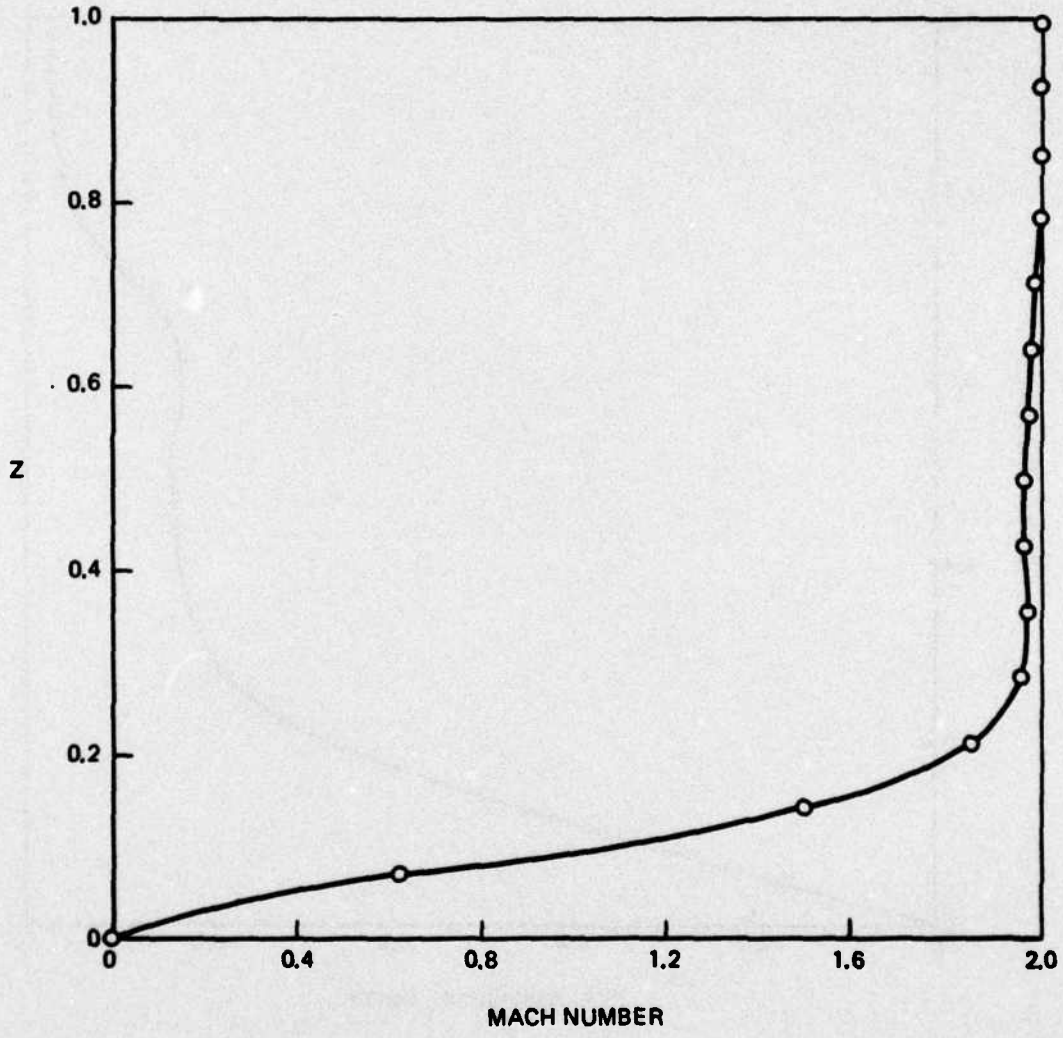

77-06-168-11

FLOW OVER A WEDGE WITH A SUPERSONIC FREE STREAM AND AN EMBEDDED SHOCK WAVE

VELOCITY PROFILE

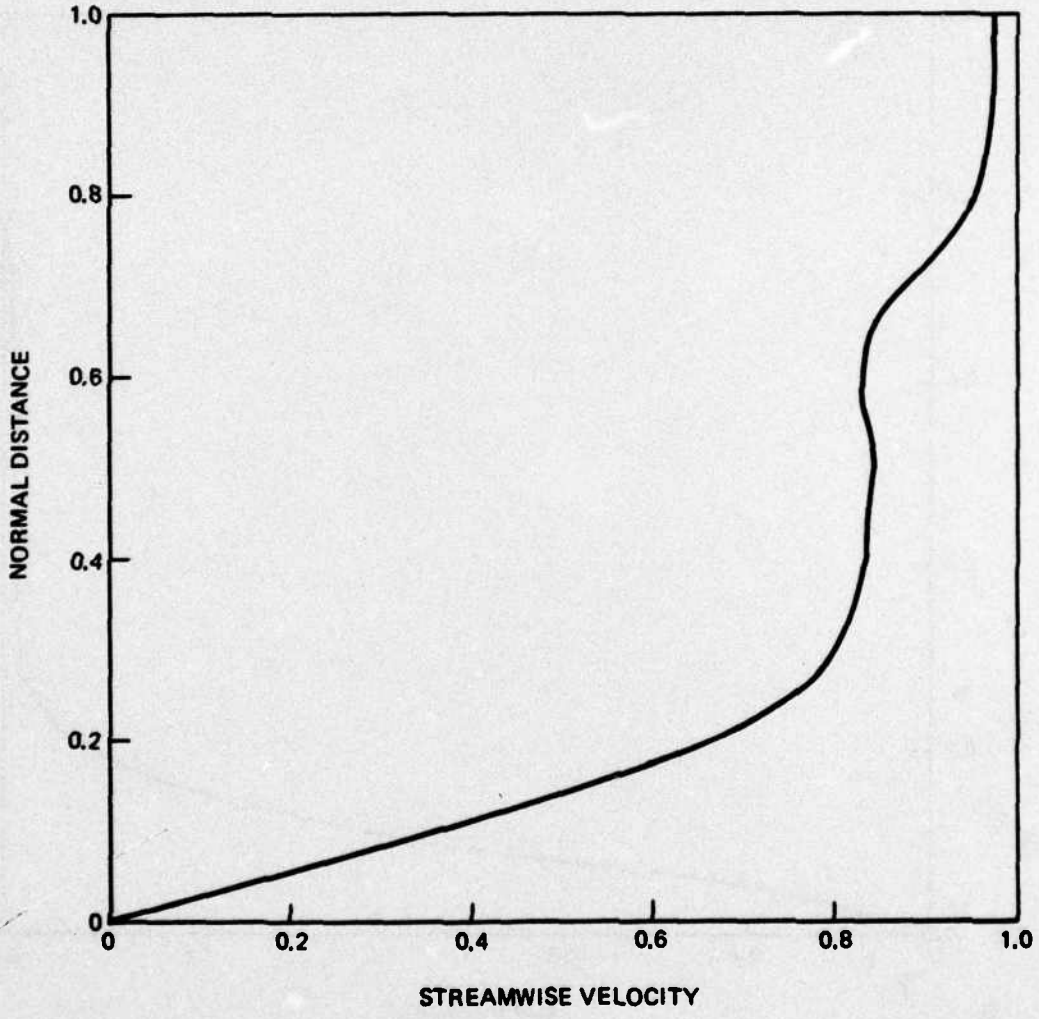

77-06-168-12

FIG. 19

FLOW OVER A WEDGE WITH A SUPERSONIC FREE STREAM AND AN EMBEDDED SHOCK WAVE

PRESSURE PROFILE

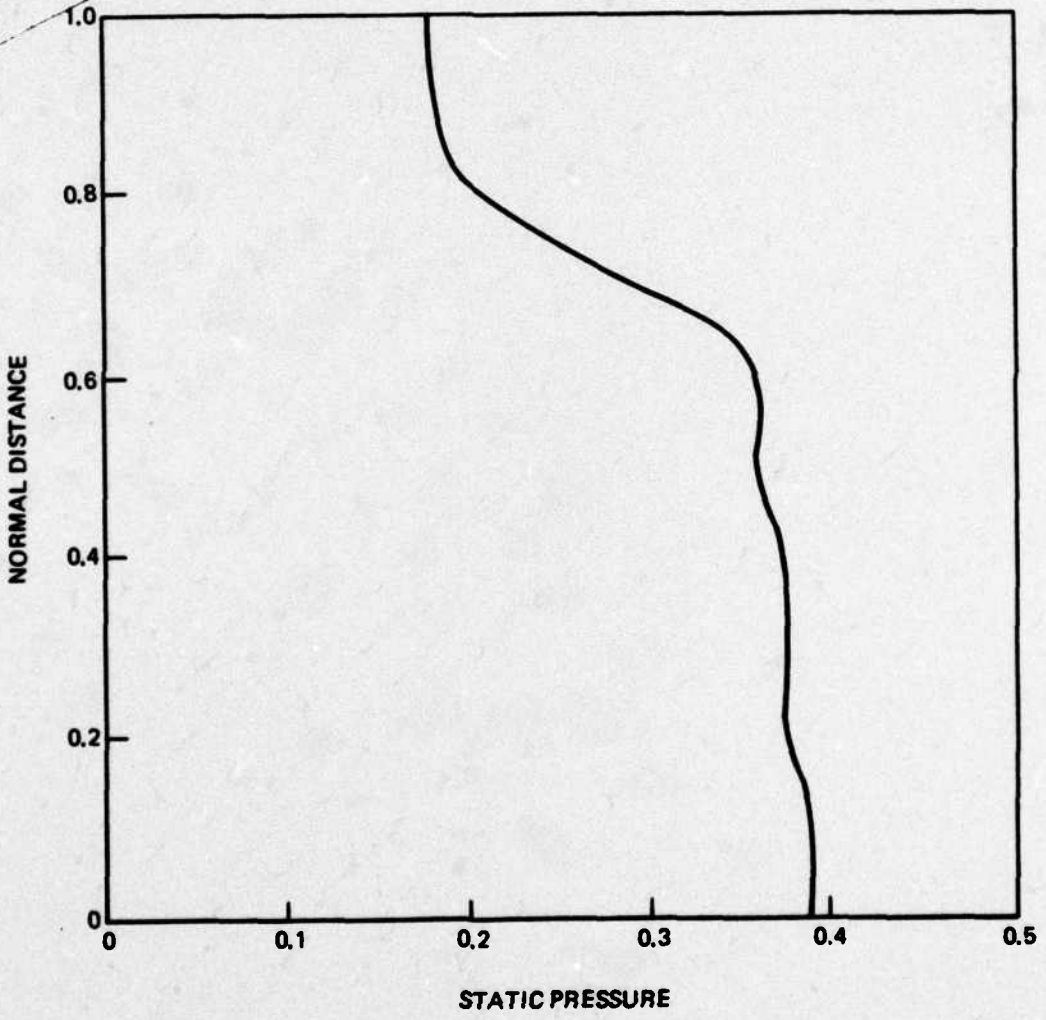

77-06-188-13

(14) UTRC-R77-912536-8

Unclassified

SECURITY CLASSIFICATION OF THIS PAGE (When Data Entered)

REPORT DOCUMENTATION PAGE

READ INSTRUCTIONS BEFORE COMPLETING FORM

1. REPORT NUMBER: R77-912536-8
2. GOVT ACCESSION NO.
3. RECIPIENT'S CATALOG NUMBER

4. TITLE (and Subtitle): A Method for Computing Flows over an Ogival Body.

5. TYPE OF REPORT & PERIOD COVERED: Final Report. Feb [redacted] 76 — Jul [redacted] 77

6. PERFORMING ORG. REPORT NUMBER

7. AUTHOR(s): P. R. Eiseman, R. Levy, H. McDonald

8. CONTRACT OR GRANT NUMBER(s): N[redacted]19-76-C-0314

9. PERFORMING ORGANIZATION NAME AND ADDRESS:
United Technologies Research Center
Silver Lane
East Hartford, CT 06108

10. PROGRAM ELEMENT, PROJECT, TASK AREA & WORK UNIT NUMBERS

11. CONTROLLING OFFICE NAME AND ADDRESS

12. REPORT DATE: Jul[redacted] 77

13. NUMBER OF PAGES: 51p.

14. MONITORING AGENCY NAME & ADDRESS (if different from Controlling Office):
Department of the Navy
Naval Air Systems Command
Arlington, VA 22217

15. SECURITY CLASS (of this report): Unclassified

15a. DECLASSIFICATION DOWNGRADING SCHEDULE

16. DISTRIBUTION STATEMENT (of this Report)

Approved for Public Release; distribution unlimited

17. DISTRIBUTION STATEMENT (of the abstract entered in Block 20, if different from Report)

18. SUPPLEMENTARY NOTES

19. KEY WORDS (Continue on reverse side if necessary and identify by block number)

Ogival Body; Tube-line coordinates; Shock Wave; Subsonic and Supersonic Flow

20. ABSTRACT (Continue on reverse side if necessary and identify by block number)

A method for computing three-dimensional flow over an ogival body at angle of attack is described. An approximate set of governing equations is given for viscous flows which have a primary flow direction. A two-level second-order accurate marching procedure is presented for general equations. With this procedure, a three-dimensional turbulent flow can be solved in any coordinate system by marching along the assumed primary flow direction. General tube-like coordinates are developed for a class of geometries applicable to flows between

DD FORM 1 JAN 73 1473 EDITION OF 1 NOV 65 IS OBSOLETE

409252

Unclassified

SECURITY CLASSIFICATION OF THIS PAGE (When Data Entered)

tubular surfaces. The coordinates are then specialized to the flow field bounded between an ogival body at angle of attack and its bow shock. Unlike the ogival body surface, the bow shock surface is not known in advance of the solution but instead must be computed as the solution develops. One marching step of the solution process is broken down into several steps. First, the bow shock surface is discretely extended by an iteration of explicit local solutions. The bow shock surface is then smoothly extended to provide a best fit to the discrete shock data. Tube-like coordinates are generated and finally the second order numerical scheme is applied to advance the fully viscous solution to the next station. In addition, some preliminary computational results were obtained. Specifically, the code was applied to subsonic boundary layers, purely supersonic flow with shocks, and mixed subsonic-supersonic flow.


DATE
ILME